Small molecule inhibitors of 25-hydroxyvitamin D-24-hydroxylase (CYP24A1): Synthesis and biological evaluation

Salvatore Ferla,[a] Ahmed S. Aboraia,[a†] Andrea Brancale,[a] Christopher J. Pepper,[b] Jinge Zhu,[c] Justin T. Ochalek,[c] Hector F. DeLuca[c] and Claire Simons[a*]

[a]*Medicinal Chemistry, School of Pharmacy and Pharmaceutical Sciences, Cardiff University, King Edward VII Avenue, Cardiff CF10 3NB, UK;* [b]*Department of Haematology, School of Medicine, Cardiff University, Heath Park, Cardiff CF14 4XN, UK;* [c]*Department of Biochemistry, University of Wisconsin-Madison, 433 Babcock Drive, Madison, WI 53706-1544, USA.*

* Corresponding author. Tel: +44-(0)-2920-876307; fax: +44-(0)2920-874149.

E-mail address: SimonsC@Cardiff.ac.uk (Claire Simons)

URL: http://www.cardiff.ac.uk/phrmy/contactsandpeople/fulltimeacademicstaff/simons-clairenew-overview_new.html

† Current address: Medicinal Chemistry Department, Faculty of Pharmacy, Assiut University, Assiut, Egypt

Abstract

The synthesis of imidazole styrylbenzamides, *tert*-butyl styrylimidazole and *tert*-butyl styrylsufonate derivatives is described. Evaluation of binding affinity and inhibitory activity against CYP24A1 identified the imidazole styrylbenzamides (**8**) as potent inhibitors of CYP24A1, and selectivity with respect to CYP27B1, comparable with or greater than the standard ketoconazole. Further evaluation of the 3,5-dimethoxy derivative (**8d**) and 3,4,5-trimethoxy derivative (**8e**) in chronic lymphocytic leukaemia (CLL) cells revealed that co-treatment of 1α,25-dihydroxyvitamin D_3 plus inhibitor coordinately upregulated GADD45α and CDKN1A. Docking experiments of the inhibitors in the CYP24A1 enzyme active site would suggest the compounds reach the active site through the vitamin D access tunnel and are exposed to multiple hydrophobic residues. The imidazole styrylbenzamides (**8**) are optimally positioned to allow interaction of the imidazole with the haem and, in the case of the methoxy derivatives, a hydrogen bond between the 3-methoxy group and Gln82 stabilises the molecule in a favourable active conformation.

Key words: (*E*)-*N*-(2-(1*H*-imidazol-1-yl)-2-phenylethyl)-4-styrylbenzamides; vitamin D receptor; CYP24A1; anti-proliferative activity; molecular modeling

INTRODUCTION

The active form of vitamin D_3, 1α,25-dihydroxyvitamin D_3 ($1,25(OH)_2D_3$, calcitriol) (Figure 1), has a multifaceted role in human physiology including regulation of calcium and phosphate homeostasis and mobilisation of bone mineral,[1] immunology through its influence on cytokine production,[2] cell proliferation and regulation of gene transcription.[3] Reduction of circulating calcitriol is associated with several diseases such as cancers,[4-6] autoimmune dysfunction[7,8] and chronic kidney disease.[9,10] This reduction in circulating calcitriol is concomitant with upregulation or overexpression of the cytochrome P450 enzyme 25-hydroxyvitamin D-24-hydroxylase (CYP24A1) responsible for the inactivation, through metabolic hydroxylation, of calcitriol and 25-hydroxyvitamin D_3 ($25(OH)D_3$).[11]

Inhibition of CYP24A1 is therefore an attractive strategy to overcome the inhibitory effects of CYP24 on VDR regulated gene expression. Two main classes of CYP24A1 inhibitors have been described, calcitriol/vitamin D derivatives and azole inhibitors. Both classes have their challenges; calcitriol therapy is limited by hypercalcaemia and this side-effect can be associated with vitamin D derivatives, whereas for the azole inhibitors the challenge is selectivity for CYP24A1 over the other major vitamin D_3 metabolising enzyme CYP27B1. Success in developing vitamin D derivatives with reduced hypercalcaemic effects have been reported[12,13] and includes the sulfone CTA018[9,12] and sulfoximine CTA091,[9,13] sulfonate TS17,[14] imidazole VIMI and cyclopropylamine CPA1[15] (Figure 1).

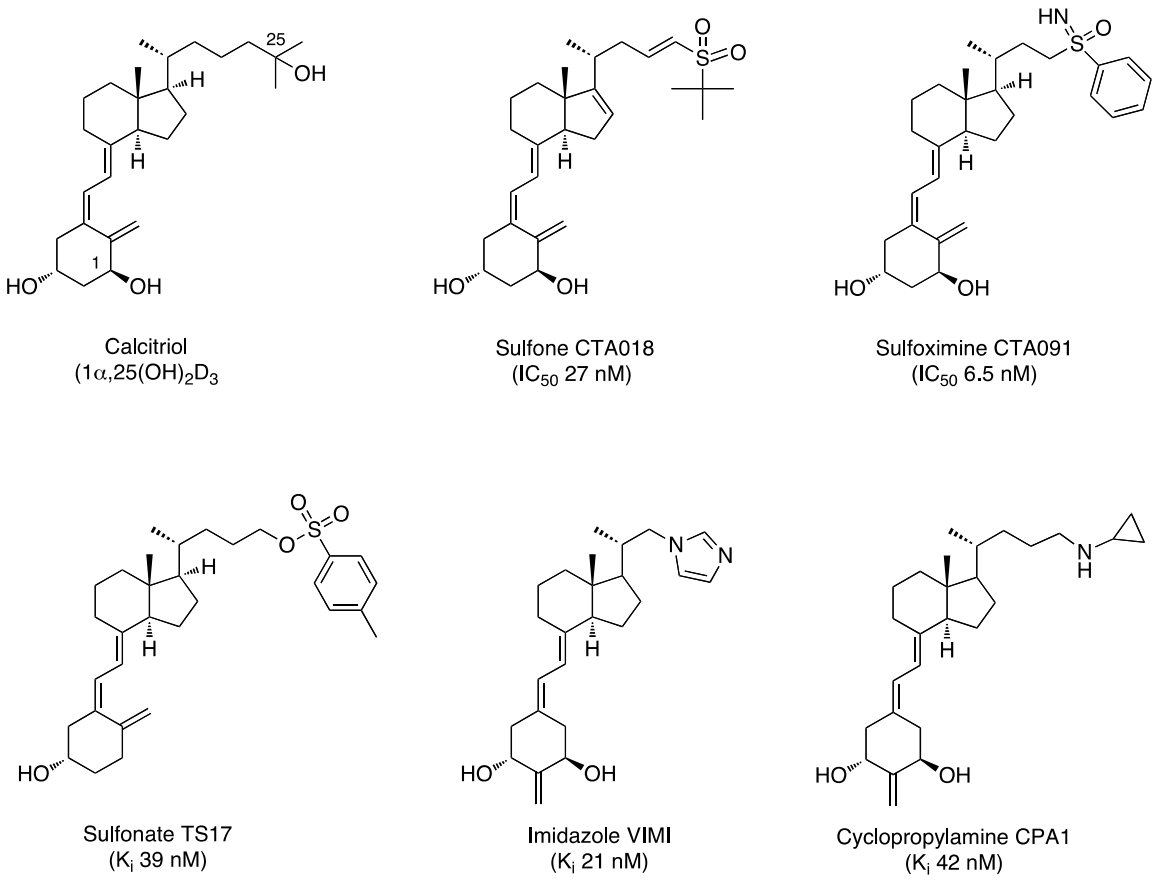

Figure 1. Reported vitamin D-like CYP24A1 inhibitors

Although the standard used for comparison in all the CYP24A1 inhibitor publications is the azole ketoconazole (Figure 2), there are fewer published reports for the azole CYP24A1 inhibitors. Ketoconazole, a broad spectrum CYP inhibitor is an azole compound with CYP24A1 inhibitory activity and approximately 4-fold selectivity for CYP24A1 *vs* CYP27B1 reported.[16] Schuster *et al.*[17] described the azole compound (*R*)-VID400 (Figure 2), which displayed a 40-fold selectivity for CYP24A1 over CYP27B1. The non-selective CYP inhibitor liarozole (Figure 2) has been shown to prolong the half-life of calcitriol and enhance up-regulation of vitamin D receptor (VDR) in DU 145 prostate cancer cell line.[18]

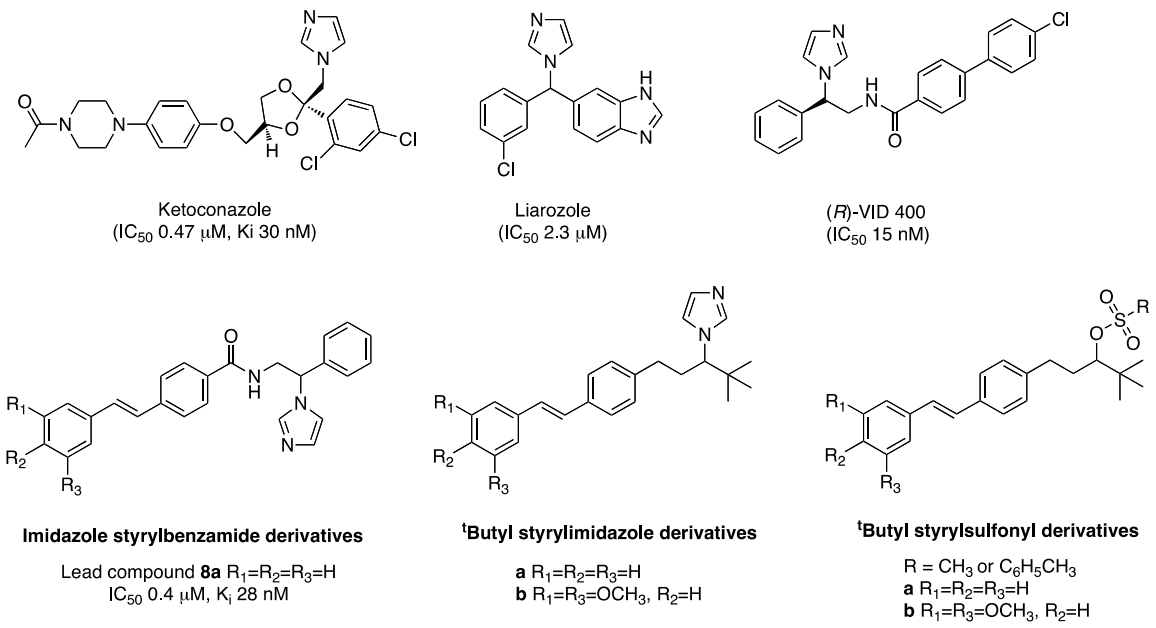

Figure 2. Azole CYP24A1 inhibitors and target compounds

This manuscript describes SAR studies on the potent imidazole styrylbenzamides previously described by us,[19] *tert*-butyl styrylimidazole and *tert*-butyl styrylsufonate derivatives (Figure 2), with CYP24A1 selectivity vs CYP27B1 and antiproliferative data for the most potent inhibitors. The substitution of the phenyl ring of the imidazole styrylbenzamides was investigated; in addition the effect of maintaining the C25 *tert*-butyl terminal of calcitriol in the styrylbenzamides with inclusion of either an imidazole (*c.f.* VIMI, Figure 1) or sulfonate (*c.f.* TS17, Figure 1) haem-binding motif was explored.

RESULTS

Chemistry. The styrenes (**2**) were prepared by Wittig reaction of the corresponding aldehyde (**1**) with methyltriphenylphosphonium bromide and potassium *tert*-butoxide following described methodology.[20] Heck reaction of the styrenes (**2**) with

4-bromobenzoic acid (**3**) produced the 4-[(*E*)-2-phenyl-1-ethylenyl]benzoic acids (**4**).[19,21-23] The synthesis of the (*E*)-4-*N*-(2-(1*H*-imidazol-1-yl)-2-phenylethyl)styrylbenzamides (**6**) was carried out using 1,1'-carbonyldiimidazole (CDI) with 2-amino-1-phenyl-ethanol (**5**) (Scheme 1).

The 4,5-dihydro-1,3-oxazoles (**7**) were prepared by the reaction of the styrylbenzamides (**6**) with methanesulphonyl chloride and a triethylamine at room temperature for 24 h.[19,24,25] In the last step of the reaction scheme, heating the oxazole compound (**7**) in the presence of imidazole opened the oxazole ring by nucleophilic displacement (Scheme 1).[19,26] A good yield of compound (**8a**-**8e**) was produced after purification by column chromatography. Catalytic hydrogenation of compound **8b**, using Pd/C 10% wt under H_2 atmosphere in THF, gave the reduced derivative **8f** (Scheme 1).

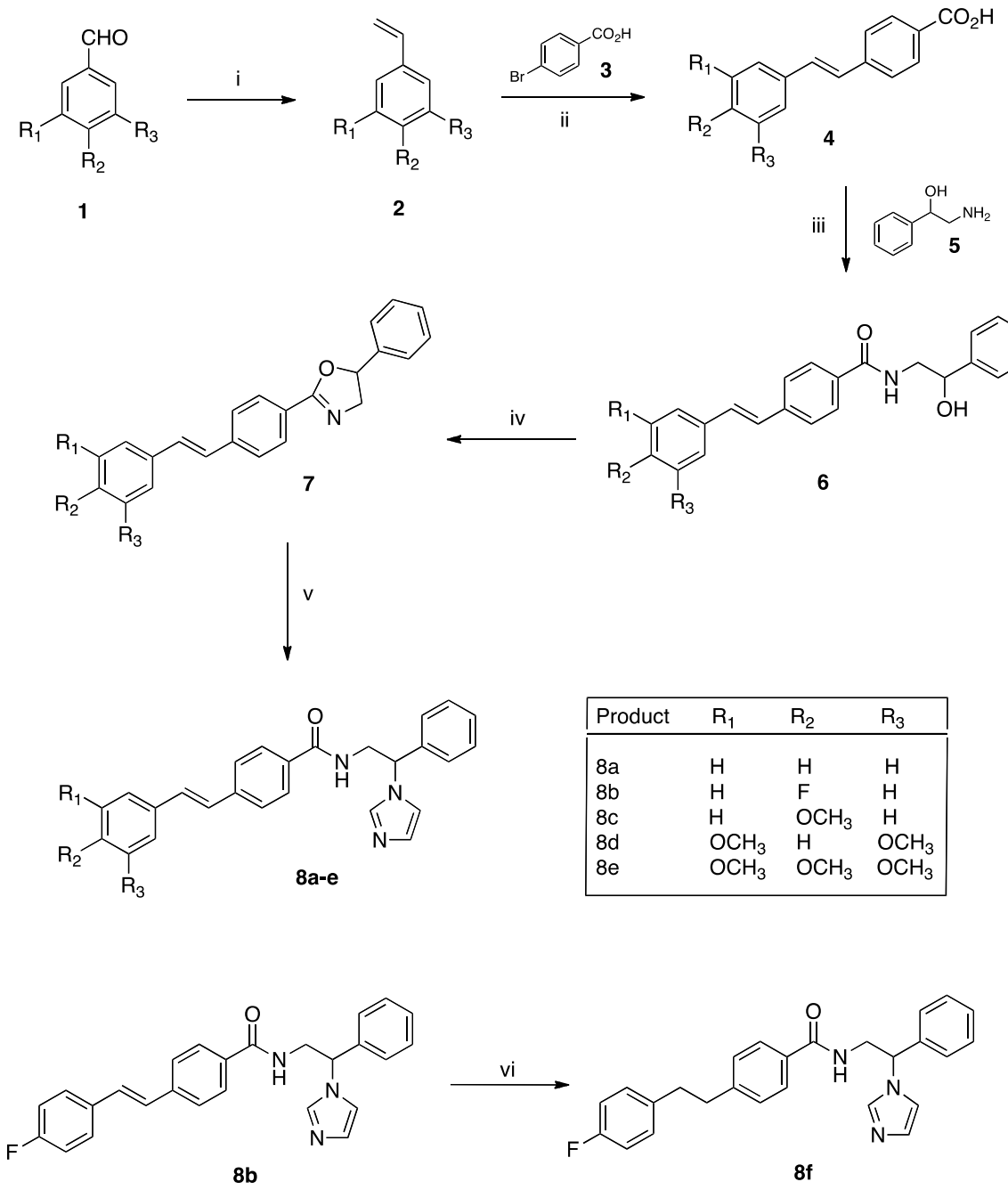

Product	R_1	R_2	R_3
8a	H	H	H
8b	H	F	H
8c	H	OCH_3	H
8d	OCH_3	H	OCH_3
8e	OCH_3	OCH_3	OCH_3

Scheme 1. *Reagents and Conditions*: (i) $PhCH_3Br$, ^tBuOK, 3 h (ii) 4-bromobenzoic acid (**3**), $Pd(OAc)_2$, ToP, Et_3N, 100 ^oC, 20 h (iii) 2-amino-1-phenyl-ethanol (**5**), CDI, 20 h (iv) CH_3SO_2Cl, Et_3N, 24 h (v) imidazole, isopropyl acetate, 125 °C, 48 h (vi) Pd/C 10% wt, H_2 atmosphere, THF, 72 h.

4-(*N*-Phenyl)-sulfamoyl benzoic acid **(9)**, prepared using a reported method[27] for the sulphonamide preparation reacting aniline and 4-(chlorosulfonyl) benzoic acid in pyridine at 0 °C and then overnight at room temperature, was reacted with 1-amino-2-phenyl ethanol (**5**) to form the amidic bond, following the method previously quoted, producing the phenylsulfamoyl-benzamide derivative **(10)**. The 4,5-dihydro-1,3-oxazole (**11**) was prepared from compound **10** as reported above, and the excess of methanesulphonyl chloride mesylated the nitrogen of the sulphonamide bond. Introduction of the imidazole ring in the lateral chain was achieved by reaction of the oxazole **(11)** in isopropylacetate in the presence of excess imidazole. An excess of imidazole was added in order to act as base and remove the mesyl protection of the nitrogen, obtaining compound (**12**) (Scheme 2).

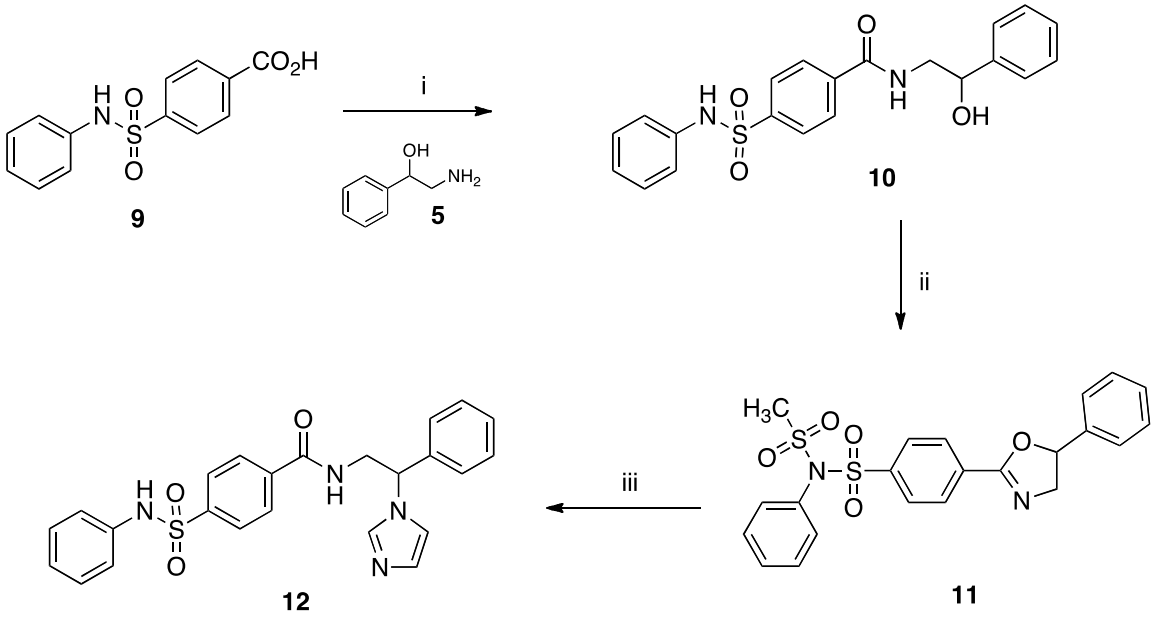

Scheme 2. *Reagents and Conditions*: (i) 2-amino-1-phenyl-ethanol (**5**), CDI, 20 h (ii) CH_3SO_2Cl, Et_3N, 24 h (iii) imidazole, isopropyl acetate, 125 °C, 48 h.

Heck reaction of the styrenes (**2**) with 1-(4-bromophenyl)-4,4-dimethylpentan-3-one (**15**), prepared by the reaction of 1-bromo-4-(bromomethyl)benzene (**13**) and 1-(*tert*-butylvinyloxy)trimethylsilane (**14**) catalyzed by indium (III) bromide following methodology described by Nishimoto *et al.*,[28] produced the ketones (**16a** and **16b**), which were subsequently reduced to the corresponding alcohols (**17a** and **17b**) on reaction with sodium borohydride (Scheme 3). Attempts to prepare the imidazole derivative (**19b**) by reaction of the alcohol (**17b**) using imidazole/ CDI, following our previously described methodology, led to isolation of the intermediate carbonyl imidazole (**18b**) only. An alternative method to introduce the imidazole ring was to first convert the alcohols (**17a** and **17b**) to a good leaving group, which could then be displaced by the imidazole anion. To this end the alcohols (**17a** and **17b**) were converted to the mesylates (**20a** and **20b**) on reaction with methanesulfonly chloride in CH_2Cl_2 and dimethylaminopyridine (DMAP). Attempts to then displace the mesylate with the imidazole anion, generated on reaction of imidazole with sodium hydride in DMF, were unsuccessful with no reaction observed (Scheme 3). The failure of both imidazole reactions was likely owing to both steric hindrance from the bulky *tert*-butyl group and electronic factors reducing the reactivity of the CH-OH towards nucleophilic substitution.

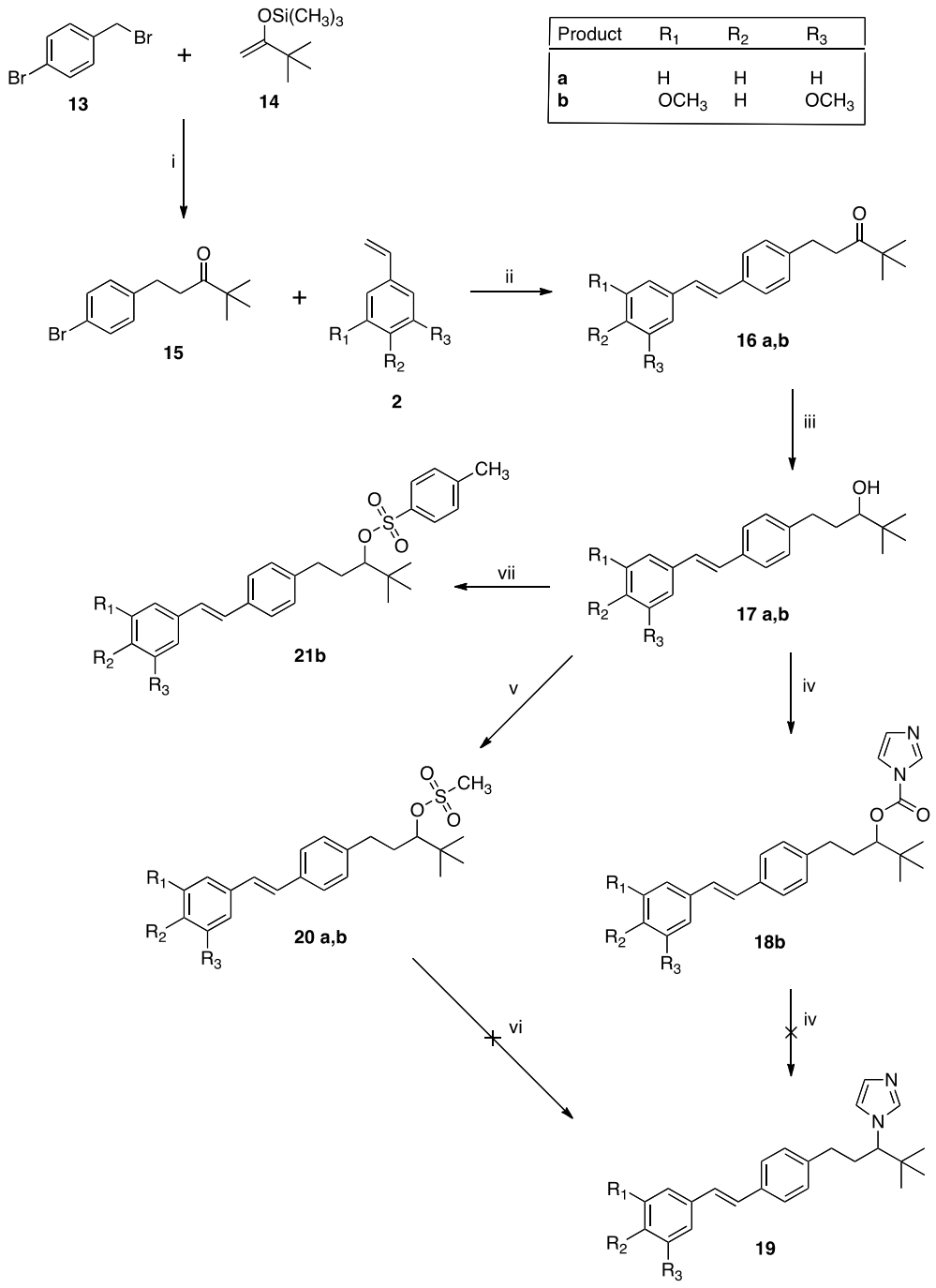

Scheme 3. *Reagents and Conditions*: (i) $InBr_3$, CH_2Cl_2, 2 h (ii) $Pd(OAc)_2$, ToP, Et_3N, 110 ^oC, 6 h (iii) $NaBH_4$, EtOH, 2 h (iv) imidazole, CDI, CH_3CN, 70 °C, 48 h (v) CH_3SO_2Cl, DMAP, CH_2Cl_2, 24 h (vi) NaH, imidazole, DMF, 45 ^oC, 24 h (vii) 4-toluenesulfonyl chloride, DMAP, CH_2Cl_2, reflux, 24 h. [**a** $R_1 = R_2 = R_3 = H$; **b** $R_1 = R_3 = OCH_3$, $R_2 = H$]

The sulfonates (**20a** and **20b**) were however of interest as potential inhibitors and in addition a tosylate derivative (**21b**) was also prepared for biological evaluation, however, unlike the mesylates, the tosylate (**21b**) was obtained in very low yield even after extensive heating with mainly starting material recovered. The failure of the tosylate reaction to reach completion could again be owing to steric hindrance by the lateral *tert*-butyl group reducing nucleophilic attack by the more bulky tosyl group compared with the smaller mesyl group.

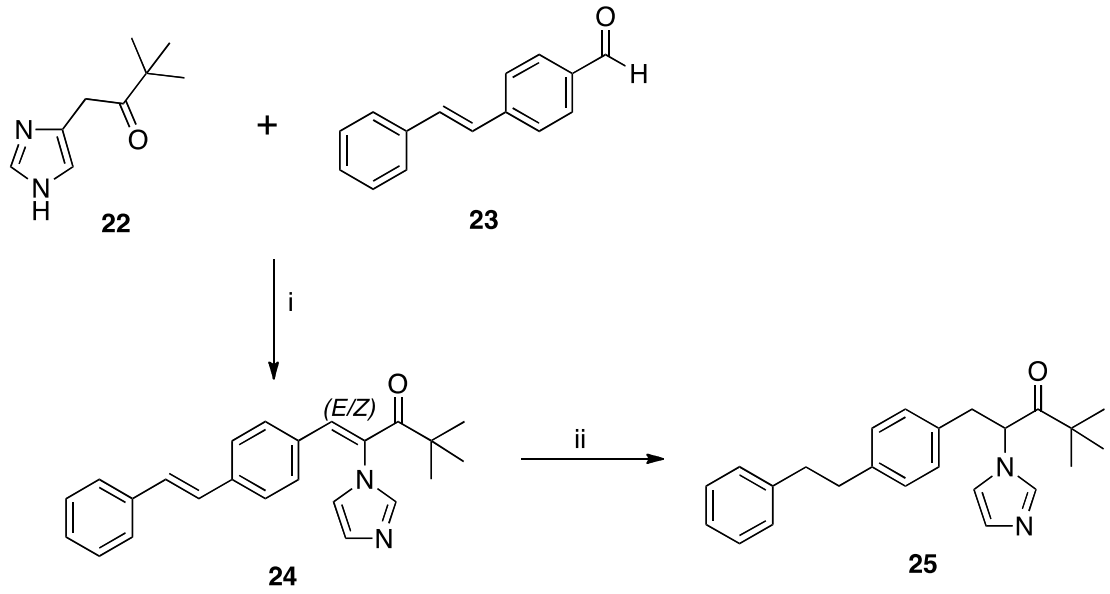

Scheme 4. *Reagents and Conditions*: (i) K_2CO_3, Ac_2O, 3 h (ii) Pd/C 10% wt, H_2 atmosphere, THF, 72 h

Minor changes in the *tert*-butyl styrylimidazole derivatives involved moving the imidazole ring from the third lateral carbon to the second and introducing a double bond in the lateral chain to introduce rigidity to the structure (Scheme 4). The lateral imidazole-*tert*-butyl chain **(22)** was easily prepared reacting imidazole, sodium hydride

and 1-bromopinacolone in DMF following the method reported by Todory *et al.*[29] The 4-styryl-benzaldehyde (**23**) was obtained via Heck reaction of styrene with 4-bromobenzaldehyde. Aldol condensation between **22** and **23** using K_2CO_3 as base in acetic anhydride gave the desired (*E/Z*)-2-imidazol-1-yl-4,4-dimethyl-1-(4-styryl-phenyl)-pent-1-en-3-one **(24)** as mixture of E/Z isomers. Catalytic hydrogenation of **24** produced the 2-imidazol-1-yl-4,4-dimethyl-1-(4-phenylethyl)-pentan-3-one **(23)** (Scheme 4).

CYP24A1 enzyme inhibition. The CYP24A1 enzymatic assay followed methodology previously described,[14] in short human CYP24A1 with an N-terminal fusion to maltose binding protein (MBP) was overexpressed in *Escherichia coli* and purified to homogeneity. The hydrolase activity was reconstituted *in vitro*, and the resulting cell-free assay system applied in the screening of the compounds to measure K*i* and IC_{50} (Table 1).

The imidazole styrylbenzamide derivatives **8** were the most active with optimal activity observed for the 3,5-dimethoxy and 3,4,5-trimethoxy substitution (**8d**, K*i* 7.8 nM, IC_{50} 0.11 μM; **8e**, K*i* 9.7 nM, IC_{50} 0.14 μM). Reduction of the styrene double bond resulted in a decreased activity (**8f**, K*i* 36 nM, IC_{50} 0.51 μM) and replacing the double bond with a sulphonamide group resulted in a more notable reduction in activity (**12**, K*i* 91 nM, IC_{50} 1.3 μM). Replacing the imidazole with sulphonates (**20** and **21**) resulted in a substantial loss in activity, likewise the keto *tert*-butyl derivative **16** also displayed poor inhibitory activity compared with the standard ketoconazole (K*i* 33 nM, IC_{50} 0.47 μM). Interestingly the intermediate carbonyl imidazole derivative **18b** showed inhibitory activity (**18b**, K*i* 11 nM, IC_{50} 0.16 μM) comparable with the imidazole styrylbenzamide

derivatives **8**. Moving the position of the imidazole group from position three to position 2 of the lateral chain resulted in good inhibitory activity for the styryl derivative (**24**, K*i* 13 nM, IC_{50} 0.18 μM) however when the alkene bonds were reduced introducing flexibility inhibitory activity was decreased (**25**, K*i* 42 nM, IC_{50} 0.6 μM).

Table 1. IC_{50} and K_i data vs CYP24A1 and CYP27B1

Compound	CYP24A1		CYP27B1		Selectivity
	IC_{50} (μM)	K_I (μM)	IC_{50} (μM)	K_I (μM)	K_I (CYP27B1/CYP24A1)
8a	0.40	0.028 ± 0.006	0.50	0.080 ± 0.005	2.8
8b	0.26	0.019 ± 0.003	0.60	0.097 ± 0.015	5.1
8c	0.34	0.024 ± 0.003	0.24	0.040 ± 0.009	1.7
8d	0.11	0.0078 ± 0.0008	0.16	0.026 ± 0.002	3.3
8e	0.14	0.0097 ± 0.0012	0.33	0.053 ± 0.006	5.5
8f	0.51	0.036 ± 0.004	0.28	0.045 ± 0.004	1.2
12	1.3	0.091 ± 0.021			
16b	2.1	0.15 ± 0.04		0.13	0.89
18b	0.16	0.011 ± 0.002	0.20	0.033 ± 0.006	3.0
20a	5.6	0.40 ± 0.02			
20b	5.4	0.38 ± 0.07		0.13	0.34
21b	2.9	0.21 ± 0.04			
24	0.18	0.013 ± 0.001	0.036	0.0057 ± 0.0004	0.44
25	0.60	0.042 ± 0.003	0.23	0.037 ± 0.004	0.88
Ketoconazole	0.47	0.033	0.36	0.058	1.7

CYP27B1 enzyme inhibition. Inhibition assay of CYP27B1 was performed in a similar way to the CYP24A1 assay as previously described,[14] and the resulting cell-free assay system applied in the screening of the compounds to measure K*i* and IC_{50} (Table 1). Compounds with good binding and inhibitory activity against CYP24A1 also displayed similar properties against CYP27B1. Selectivity similar or greater than the standard, ketoconazole (selectivity CYP27B1/CYP24A1 = 1.7) was observed for most of the compounds, most notably the styryl imidazoles **8b** and **8e** had 5-fold selectivity for CYP24A1 over CYP27B1.

Compounds **8d** and **8e** were subject to further evaluation to determine effect on CLL cells and vitamin D receptor (VDR) genes.

Effects of 1,25-$(OH)_2D_3$ and CYP24A1 inhibitors on CLL cells. The imidazole styrylbenzamides **8** were analysed for anti-cancer activity in primary CLL cells. Primary CLL cells were more sensitive to the effects of calcitriol when compared with normal B-cells with a mean LD_{50} of 0.28μM (Figure 3a). The differential toxicity in CLL cells versus normal B-cells can be explained by the enhanced CYP24A1 expression in CLL cells.[30] This selectivity was also observed for compound **8d** and to a much lesser extent for compound **8e** (Figure 3b, Table 2).

3a

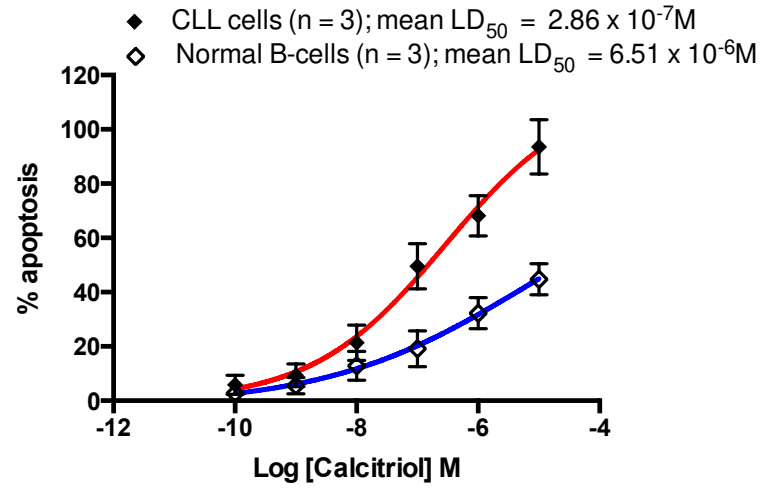

3b

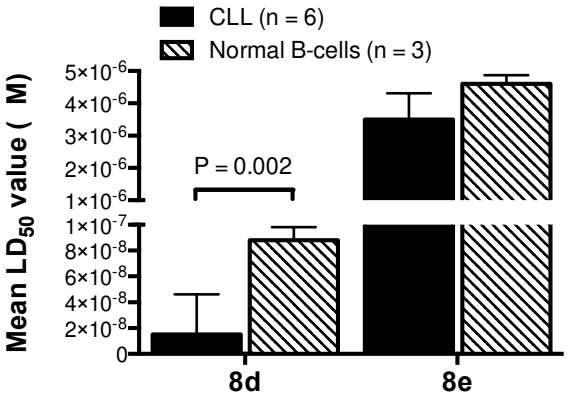

Figure 3. Apoptotic effects of calcitriol and CYP24A1 inhibitors in CLL and normal B-cells.

(a) Primary CLL cells and normal B-cells were purified by negative selection using $CD3^+$ Dyanbeads. Cells were then cultured for 48h in the presence of calcitriol (0-10μM) and apoptosis was assessed using Annexin V/propidium iodide labelling and quantified by flow cytometry. CLL cells were >20 times more sensitive to the effects of calcitriol when compared with normal B-cells. **(b)** Primary CLL cells were treated with the CYP24A1

inhibitors **8d** and **8e** for 24h. Furthermore, **8d** was selectively toxic to CLL cells when compared to normal B-cells following incubation with CYP24A1 inhibitor for 48h.

The *in vitro* cytotoxicity of the novel CYP24 inhibitors was evaluated in primary CLL cells (n = 6) (Table 2). Experiments were performed in duplicate and the LD_{50} values expressed as mean (±SD) for the six samples tested. Sensitivity to fludarabine (a commonly used treatment for CLL) was assessed in the same primary leukemia cells; the data indicate that a number of the CYP24 inhibitors were more potent than fludarabine. The data obtained (Table 2) clearly show a detrimental effect of a 4-methoxy substituent (**8c** and **8e** IC_{50} 3.4 μM) on anti-cancer activity compared with the unsubstituted, 4-fluoro and 3,5-dimethoxy derivatives (**8a** IC_{50} 27 nM, **8b** IC_{50} 15 nM and **8d** IC_{50} 13 nM respectively).

Table 2. *The in vitro* cytotoxicity of the novel CYP24 inhibitors was evaluated in primary CLL cells (n = 6)

Compound	**R_1**	**R_2**	**R_3**	**LD_{50} (μM)**
8a	H	H	H	0.027 (± 0.018)
8b	H	F	H	0.015 (± 0.011)
8c	H	OCH_3	H	3.2 (± 0.14)
8d	OCH_3	H	OCH_3	0.013 (± 0.01)
8e	OCH_3	OCH_3	OCH_3	3.5 (± 0.15)
Fludarabine				1.1 (± 0.32)

Effects of 1,25-$(OH)_2D_3$ and CYP24A1 inhibitors on CLL cells. The results here showed that treatment with 10 nM 1,25-$(OH)_2D_3$ had no significant effect on GADD45α and CDKN1A mRNA expression in CLL cells compared with untreated cells (Figure 4). At 100 nM 1,25-$(OH)_2D_3$ a small enhancement was observed. However, when the cells were treated with **8d** in combination with 100 nM calcitriol the GADD45α mRNA was enhanced significantly ($P < 0.01$) and induction was dependent on inhibitor concentration with optimal enhancement observed at 0.05-0.10 μM CYP24A1 inhibitor **8d** in combination with 100 nM calcitriol (Figure 4A). Induction of CDKN1A mRNA on combination with 100 nM calcitriol/0.01-0.10 μM **8d** was also significant ($P < 0.05$) (Figure 4B). Combination of 1,25-$(OH)_2D_3$ (100 nM) with **8e** (0.05-0.10 μM) resulted in a significant ($P < 0.05$) induction of GADD45α and CDKN1A mRNA expression (Figure 4C and 4D).

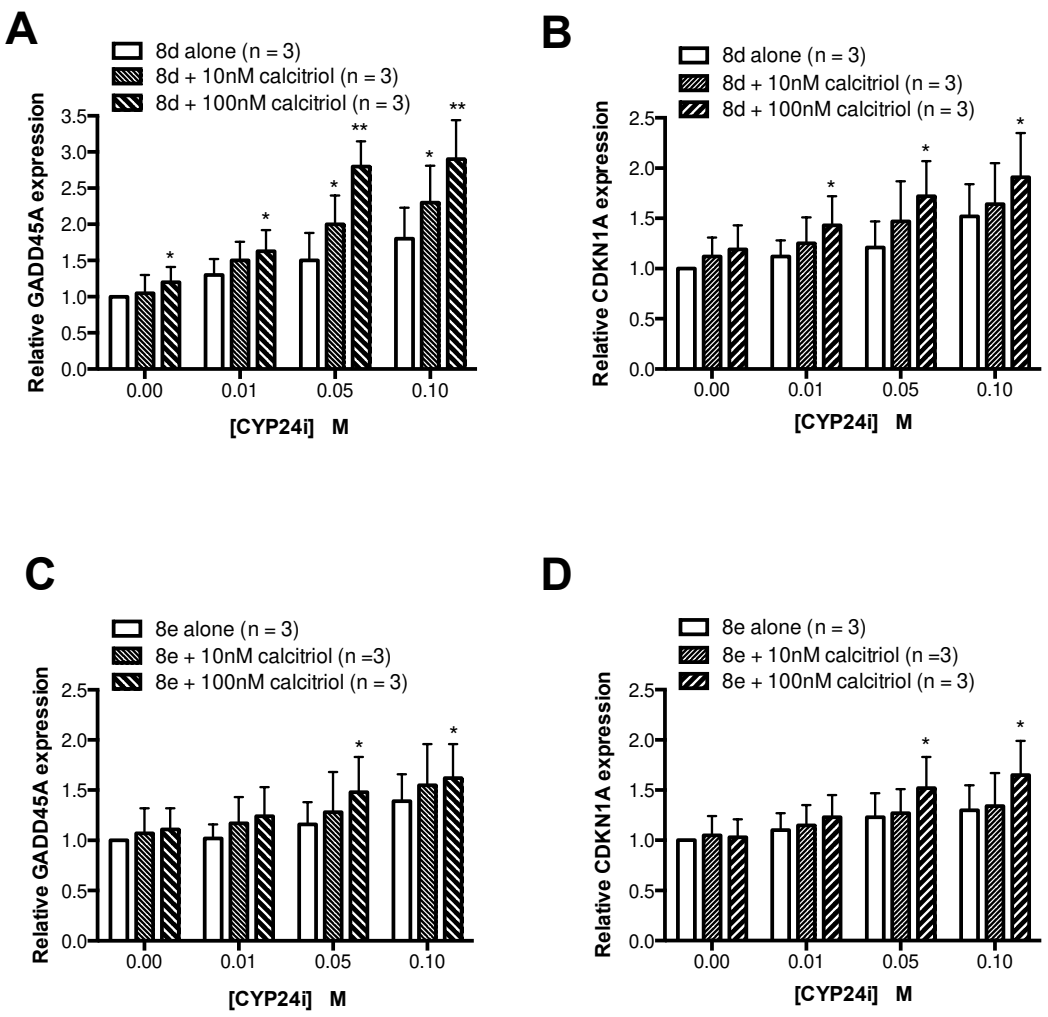

Figure 4. **CYP24A1 inhibition significantly increases the transcription of vitamin D target genes in a dose-dependent manner.**

Primary CLL cells were treated with **8d** in the presence and absence of 10nM and 100nM calcitriol for 24h. The transcription of GADD45A, CDKN1A and RPS14 (house-keeping gene) were analysed by quantitative RT-PCR on a LightCycler 2.0 instrument. Relative changes in transcription were expressed as the ratio of target gene to RPS14. **8d** caused a dose-dependent increase in relative transcription of (A) GADD45A and (B) CDKN1A. This was further enhanced in the presence of calcitriol. In contrast, **8e** did not induce

significant changes in (C) GADD45A or (D) CDKN1A unless co-administered with 100nM calcitriol. *, P<0.05; **, P<0.001.

Molecular Modeling.

Homology Model

Homology model of the human CYP24A1 was built with MOE-homology tool using a single template approach following the methodology previously reported by our group and using the Amber99 force field.[31] The crystal structure of the rat enzyme isoform (pdb ID:3K9V)[32] was used as template, considering the high sequence similarity (83%) with the human one as reported in literature.[15] The sequence of the human isoform was loaded in MOE together with the 3D structure of the rat isoform, aligned and the final 3D model was obtained as single output structure. Validation of the new model in terms of the stereochemical quality of the backbone, side chain and amino acids environment were conducted using the on-line applications RAMPAGE server, Verify 3D and Errat.[33,34,35]

DISCUSSION

The (*E*)-*N*-(2-(1*H*-imidazol-1-yl)-2-phenylethyl)-4-styrylbenzamides (**8**) were readily prepared using an efficient 5-step synthesis. The results of the CYP24A1 inhibition assay would suggest substitutions on the styryl phenyl ring are important to activity. The unsubstituted compound (**8a**) had low activity, whereas the introduction of substituents on the ring resulted in an improvement in activity up to 4-fold. Introduction of methoxy groups in positions 3 and 5 (R_1 and R_3) (**8d**) and in 3,4,5 position (**8e**) led to the best activity with a K*i* in the nM range. Substitution in the 4-position (R_2, Table 1) with F or

OCH_3 in compounds **8b** and **8c** was detrimental to activity. Hydrogenation of the styryl linker produces a decrease in activity (**8f**), which was more evident after its replacement with a sulphonamide (**12**). Although any SAR for this small series is very preliminary, molecular docking studies can provide a rational explanation for the observed enzymatic data. All the compounds reached the active site through the vitamin D access tunnel and were exposed to multiple hydrophobic residues (Ile131, Trp134, Met246, Phe249, Thr394, Thr395, Gly499, Tyr500), which have been reported having multiple hydrophobic interactions with calcitriol.[32,35] This pose allows the imidazole ring in an optimal position for the interaction between its nitrogen lone pair and the haem iron. Compounds **8d** and **8e** present an additional hydrogen bond between their 3-methoxy group and Gln82, which stabilises the two compounds in the favourable active conformation and could explain the small improvement in CYP24A1 inhibition activity (Figure 5).

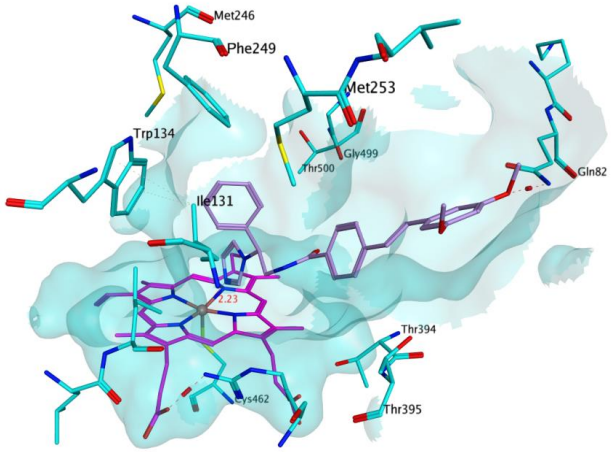

Figure 5: **Docking of 8d**: the compound occupies the access tunnel with the imidazole ring in an optimal orientation for the interaction with the iron. The hydrogen bond between its 3-methoxy group and Gln82 stabilises the molecule in a favourable active conformation.

The rest of the compound family, lacking this extra hydrogen bond, is free to move in the wide pocket and consequently their binding poses in the active site are more variable with reduced activity observed (Figure 6).

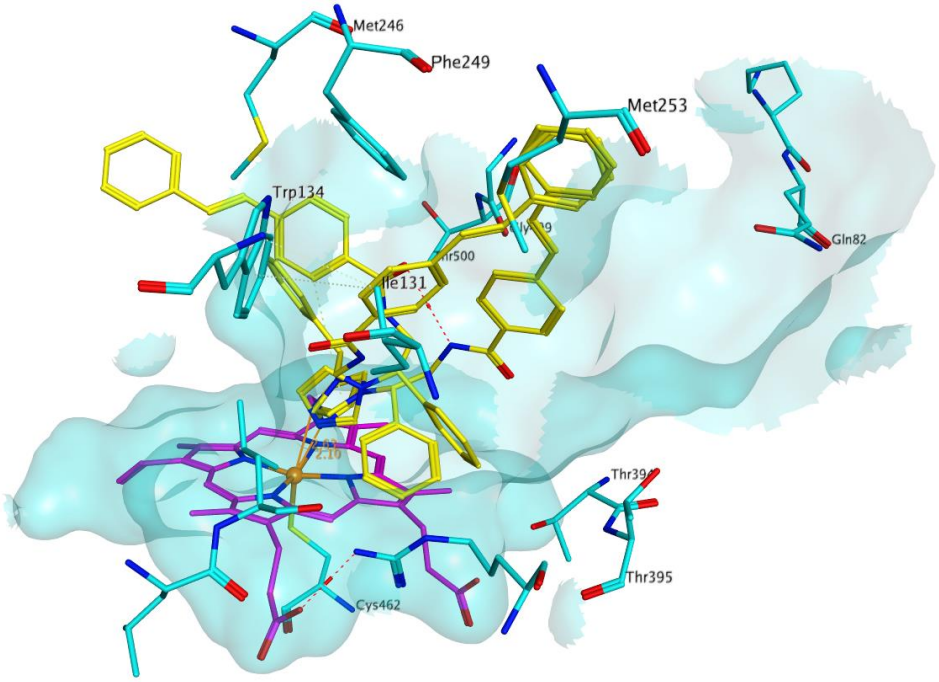

Figure 6: **Docking of 8a**: Due to the absence of hydrogen bond with Gln82, the molecule binding poses in the active site are more variable, possibly justifying the reduced activity observed for this compound.

The molecule flexibility conferred by hydrogenation of styryl linker (**8f**) or by its replacement by sulphonamide (**12**) results in a reduction in activity in the first case and a decrease of activity in the second emphasizing the importance of the structural rigidity in the active site disposition. The docking has shown how, due to the high flexibility of the sulphonamide bond, compound **12** assumes multiple possible conformations in the binding pocket and none of them allow the correct disposition in the active site (Figure

7).

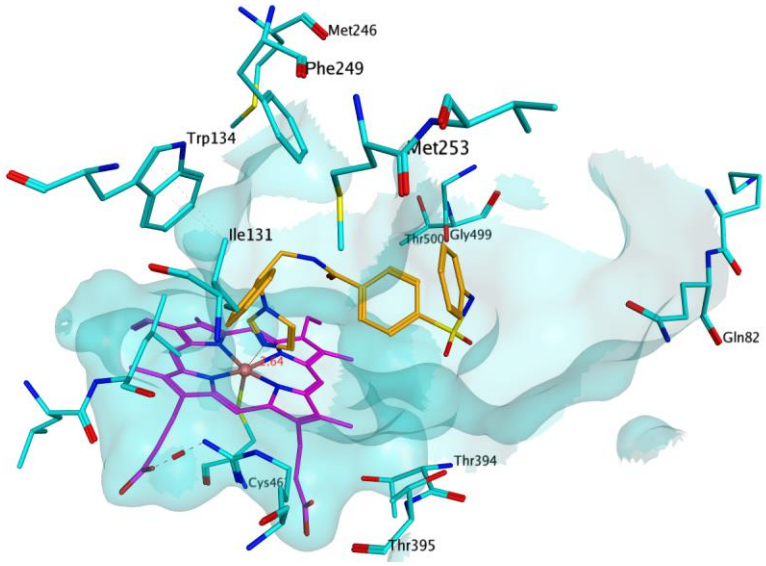

Figure 7: **Docking of 12**: Due to the high flexibility of the sulphonamide bond, compound **12** is not able to entirely occupy the access channel.

To further validate the binding mode of the docking results, 5 ns molecular dynamics (MD) studies were performed for compounds **8a-d** and **12** considering the protein flexibility and the interaction changes of ligand-protein complex during the time. The hydrophobic nature of the active site is an optimal environment for these lipophilic molecules and this could be an explanation for the stability shown by most of the different systems. Furthermore, a haem-imidazole coordination is present during all the simulation for all the derivatives, except for compound **12**, with an optimal distance Fe-N for the interaction between 2.40 and 3.85 Å (Table 3).

Table 3. Calculated ligand interaction energies for the compounds analysed by molecular dynamics.

Compound	$\Delta G_{binding}$ (Kj/mol)*	**Fe-N distance (**Å)*
8d	-19.83183	2.58
8b	-17.26674	2.40
8c	-14.52405	3.85
8a	-13.95545	2.74
12	3.49442	5.48

*Average values of $\mathbf{\Delta G_{binding}}$ and **Fe-N** distance calculated excluding the first 2ns of MD in which the system protein-ligand reached stability.

The lowest estimate $\Delta G_{binding}$ energy was found for compound **8d,** whereas compound **12** showed the highest energy value. This relation between the estimate $\Delta G_{binding}$ and the enzymatic assay results was also found for compound **8a**, **8b** and **8c** (Table 3). The best results for compound **8d** could be a consequence of the hydrogen bond with Gln82 (Graphic 1), which keeps the molecule in the right conformation for all the MD duration giving a further contribution to the system stability.

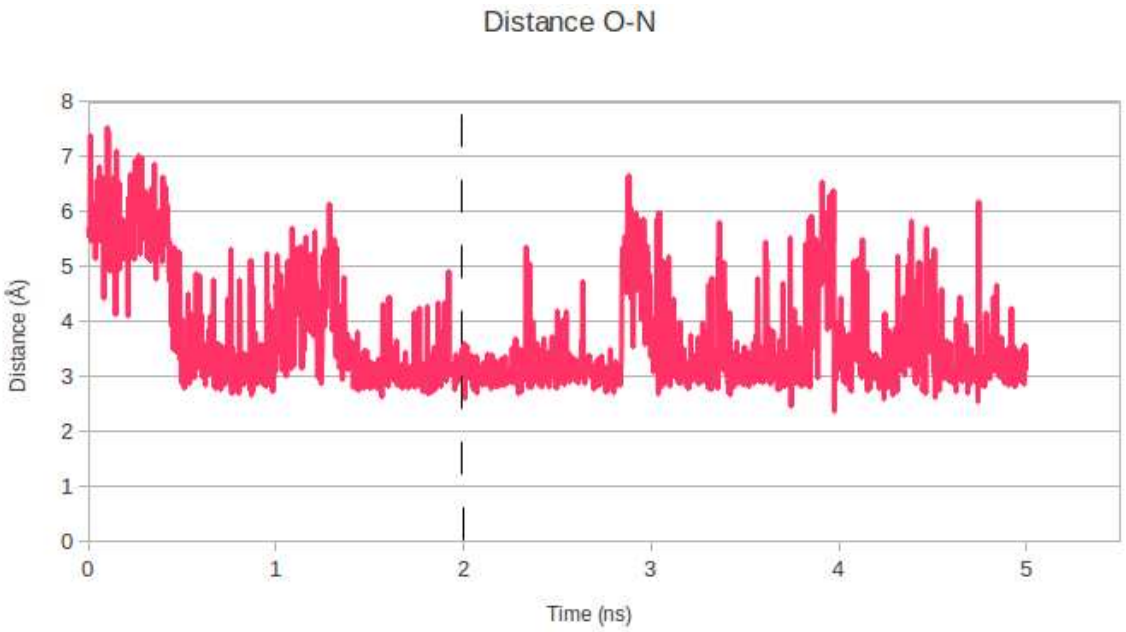

Graphic 1: Trend, during the 5ns MD simulation, of the distance O-N in the hydrogen bond formation between the 3-methoxy group of **8d** and Gln82. After 2ns of stabilization, the average distance is 3.51 Å.

The high value of energy reported for compound **12** is a consequence of the high flexibility of the sulphonamide bond. The molecule is not able to accommodate entirely in the enzyme access channel during all 5ns MD simulation. As consequence of that, compound **12** loses its imidazole-iron coordination and therefore part of its anti-CYP24A1 inhibitory activity. Graphic 2 reports the Fe-N distance trend during the 5ns MD of compound **8d** and **12**. After the system stabilization in the first 2ns, the distance remains stable for **8d**, while the distance increment for compound **12** indicates a loss of coordination to the haem.

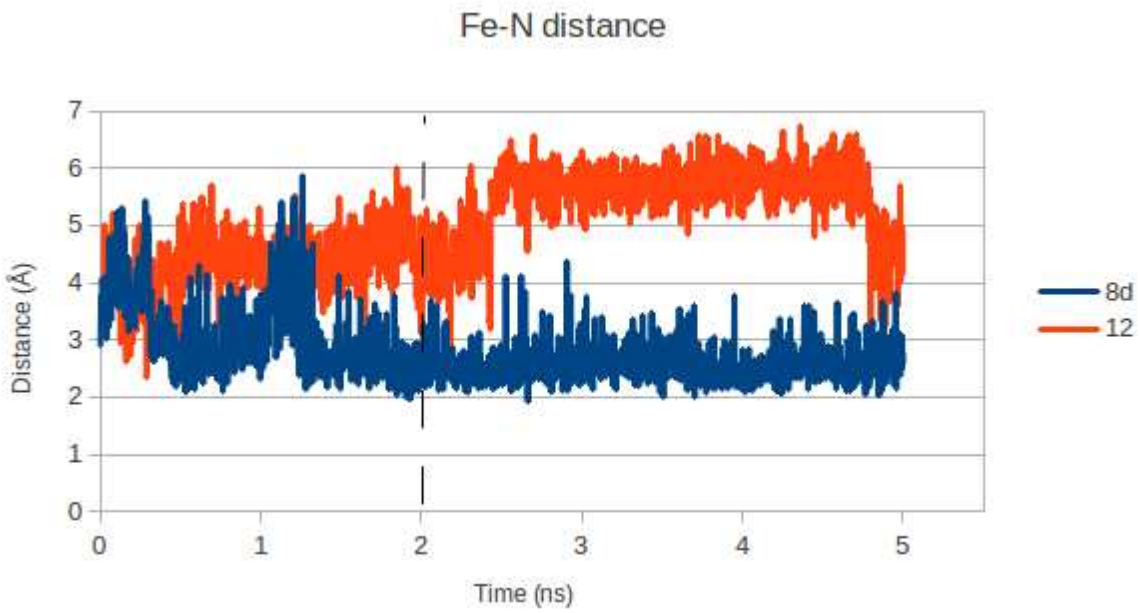

Graphic 2: Distance Fe-N trend during 5ns MD simulation. After 2ns of stabilization, the distance remains stable for **8d**, while the distance increment for compound **12** indicates a loss of coordination to the haem.

None of the sulfonate/tosylate derivatives (**20a, 20b, 21b**) showed interesting CYP24A1 activity underlining the key rule of the imidazole ring in the binding to the haem, and a further confirmation was given by the activity found for compound **18b**, **24** and **25**, in which the imidazole was present in the lateral chain. The nitrogen lone pair could be more available for the interaction with the iron if compared with the oxygen one making the sulfonate-Fe interaction weaker than imidazole-Fe resulting in an ineffective anti-CYP24A1 activity.

Further biological evaluation of two of the CYP24A1 inhibitors, (*E*)-N-(2-(1*H*-imidazol-1-yl)-2-phenylethyl)-4-(3,5-dimethoxystyryl)benzamide (**8d**) and (*E*)-N-(2-(1*H*-imidazol-1-yl)-2-phenylethyl)-4-(3,4,5-trimethoxystyryl)benzamide (**8e**) were conducted to

determine the effect of the inhibitors of VDR target genes GADD45α and CDKN1A. Induced expression of GADD45α inhibits cell proliferation and is induced by various agents that damage DNA and arrest cell growth.[36] CDKN1A (also known as $p21^{waf1}$), a cell-cycle regulatory protein inhibits the activity of cyclin-dependent kinases in the G_0/G_1 cell-cycle phase, resulting in cell-cycle arrest. Induction of GADD45α and CDKN1A has been shown to contributes to the growth-inhibitory effects of 1,25-$(OH)_2D_3$.[37]

Co-administration of the dimethoxy derivative (**8d**) with 100 nM 1, 25-$(OH)_2D_3$ significantly enhanced the induction of GADD45α ($P < 0.01$) and CDKN1A ($P < 0.05$) (Figure 4 A/B) with optimal induction observed with a concentration of 0.05-0.10 μM of inhibitor **8d**. Co-administration of the trimethoxy derivative (**8e**) with 100 nM 1, 25-$(OH)_2D_3$ significantly enhanced the induction of GADD45α and CDKN1A ($P < 0.05$) (Figure 4 C/D) with optimal induction observed with a concentration of 0.05-0.10 μM of inhibitor **8e**. The effect on induction of both VDR target genes was significant however the effects were more marked for the combination of **8d**/1,25-$(OH)_2D_3$ compared with **8e**/1,25-$(OH)_2D_3$.

Conclusions

Optimal binding and inhibitory activity was achieved with the imidazole derivatives (**8**, **18** and **24**) and with a rigid styryl moiety. Docking and molecular dynamics experiments provide a rationale for the importance of conformational stability to allow the inhibitor to entirely occupy the access channel and coordinate with the haem. The 3-methoxy group in compounds **8d** and **8e** presents an additional hydrogen bond between their 3-methoxy

group and Gln82, which stabilises the two compounds in the favourable active conformation with an improvement in CYP24A1 inhibitory activity.

Modest CYP24A1 *vs* CYP27B1 selectivity was achieved with the imidazole styrylbenzamides (**8**) with > 5-fold selectivity observed for the 4-fluoro and 3,4,5-trimethoxy derivatives, **8b** and **8d**, respectively, which was an improvement compared with the 1.7-fold selectivity observed for ketoconazole (Table 1). The nanomolar inhibitory activity and modest selectivity of the imidazole styrylbenzamides (**8**) combined with the significant induction of VDR target genes GADD45α and CDKN1A in primary chronic CLL cells provides useful lead compounds for further development.

EXPERIMENTAL SECTION

General Procedures. 1,25$(OH)_2D_3$ and 25$(OH)D_3$ were purchased from SAFC-Pharma (Madison, WI). Human MBP-CYP24A1, mouse CYP27B1, bovine adrenodoxin (Adx), and adrenodoxin reductase (AdR) were purified as described previously.[14]

^1H and ^{13}C NMR spectra were recorded with a Brucker Avance DPX500 spectrometer operating at 500 and 125MHz, with Me_4Si as internal standard.Mass spectrometry data was acquired at the EPSRC UK National Mass Spectrometry Facility at Swansea University. Microanalyses were determined by Medac Ltd (Surrey, UK). Flash column chromatography was performed with silica gel 60 (230-400mesh) (Merck) and TLC was carried out on precoated silica plates (kiesel gel 60 F_{254}, BDH). Melting points were determined on an electrothermal instrument and are uncorrected. Compounds were visualised by illumination under UV light (254 nm) or by the use of vanillin stain followed by charring on a hotplate. All solvents were dried prior to use as described by

the handbook Purification of Laboratory Chemicals[38] and stored over 4Å molecular sieves, under nitrogen. All compounds were more than 95% pure.

The benzoic acids (**4**) were prepared according to literature methods[19,20-22] and the synthesis of (**8a**) was previously reported.[19]

CYP24A1 inhibition assay.

Inhibition of CYP24A1 was carried out as described previously.[14] Briefly, reaction mixture containing 0.1 μM each of Adx and AdR, 0.075 μM MBP-CYP24A1, 2.5 μM $1,25(OH)_2D_3$, varying concentrations of inhibitors, and 0.5 mM NADPH was incubated at 37 °C for 25 min in a buffer of 20 mM Tris (pH 7.5) and 125 mM NaCl. All inhibitors were dissolved in ethanol (>10 mM) or DMSO (>50 mM) and further diluted in ethanol to make working stock (<1 mM). The reaction was extracted with CH_2Cl_2 and analyzed by HPLC. The IC_{50} values were determined by fitting the relative activity (V/V_0) against the inhibitor concentration [I] using the equation $V/V_0 = IC_{50}/(IC_{50} + [I])$, where V and V_0 are the reaction rates in the presence and absence of inhibitors. The K_I values were calculated using equation $K_I = IC_{50}/(1 + [S]/K_M)$, where [S] is the substrate concentration and K_M = 0.19 μM.[14]

CYP27B1 inhibition assay.

Inhibition assay of CYP27B1 was performed in a similar way to that of CYP24A1 as previously described.[14] The concentration of substrate $25(OH)D_3$ was 2.5 μM and K_M for CYP27B1 was 0.48 μM.

Cell culture conditions

Freshly isolated peripheral blood lymphocytes ($1x10^6$/ml) were cultured in RPMI medium (Invitrogen) supplemented with 100 units/ml penicillin, 100 μg/ml streptomycin,

10% fetal calf serum and 5ng/ml IL-4. Both CLL cells and normal B-cells were purified by negative selection using $CD3^+$ Dyanbeads (Invitrogen); purity was assessed by flow cytometry and only samples with >90% target cells were used in subsequent experiments. Lymphocytes were incubated at 37^{o}C in a humidified 5% carbon dioxide atmosphere in the presence of CYP24 inhibitors (0 – $1x10^{-7}$M) and/or calcitriol (0 - $1x10^{-5}$M) for up to 48h. In addition, control cultures were set up in which no drug was added to normal and leukaemic lymphocytes. Cells were subsequently harvested by centrifugation and were analyzed by flow cytometry using the methods outlined below. Experiments were performed either in duplicate or triplicate.

Measurement of *in vitro* apoptosis

Cells were harvested and then resuspended in the supplied binding buffer according to the manufacturer's instructions (Bender Medsystems). Subsequently, 4µl of fluorescein-labelled Annexin V was added to each aliquot of cells in then incubated in the dark for 10 mins. Cells were then washed and resuspended in binding buffer with 10µl propidium iodide. Apoptosis was quantified on an Accuri C6 flow cytometer (Becton Dickinson) and analysed using CFlow software. LD_{50} values were calculated from the sigmoidal dose-response curves using Prism 6.0 software (Graphpad). All experiments were performed in triplicate.

RT-PCR analysis of GADD45A and CDKN1A transcription

$1x10^7$ CLL lymphocytes and normal B-lymphocytes were incubated with 8d and 8e (0, 0.01, 0.05 and 0.1µM) for 24h in the presence or absence of calcitriol (10nM and 100nM). Cells were harvested and total RNA was extracted from using RNeasy spin

columns according to the manufacturer's instructions (Qiagen, Crawley, UK). One microgram of total RNA was then reverse transcribed using a Clontech first strand cDNA synthesis kit (Clontech, Between Towns, UK). Subsequently real time PCR was performed using gene-specific primers for GADD45A, CDKN1A and ribosomal protein RPS14 (house-keeping gene) in PCR buffer containing 50nM of each primer, 4.0 mM $MgCl_2$ cDNA template and FastStart SYBR Green I DNA master mix (Roche Diagnostics, UK) in a 10 µl final volume. Each reaction was cycled 35 times consisting of 10 sec denaturation (95^{o}C), 5 sec annealing (60^{o}C) and 20 sec extension (72^{o}C) on a Roche LightCycler 2.0 instrument (Roche Diagnostics). The amount of RPS14 mRNA was quantified in all samples as an internal house-keeping control and SYBRGreen was used as the detection method. The results of the real-time RT-PCR were expressed as normalised target gene values, e.g. the ratio between GADD45A and RPS14 transcripts calculated from the crossing points of each gene. All experiments were performed in duplicate. The gene-specific primer pairs used were as follows:

GADD45A:

Forward primer sequence: GCAGGATCCTTCCATTGAGA

Reverse primer sequence: CTCTTGGAGACCGACGCTG

CDKN1A:

Forward primer sequence: CATGGGTTCTGACGGACAT

Reverse primer sequence: AGTCAGTTCCTTGTGGAGCC

RPS14 (house-keeping gene):

Forward primer sequence: GGCAGACCGAGATGAACTCT

Reverse primer sequence: CCAGGTCCAGGGGTCTTGGT

Molecular Modelling

Docking studies were performed using LeadIT2.1.2 docking program by BioSolve.IT.[39] The important amino acid residues of the active pocket (Gln82, Ile131, Trp134, Met246, Ala326, Glu329, Thr330, Val391, Phe393, Thr394, Ser498, Gly499, Tyr500)[32] were selected and then the selection was extended to 12 Å in order to include in the docking site the haem iron region and the access tunnel to the catalytic site. A ligands database in mol2 format, prepared using MOE,[40] was used as input for the docking calculations. The iron atom of the catalytic site was set as essential pharmacophoric feature. Ligand docking was performed using the default values and no water molecules were considered. Ten output solutions were obtained from each compound and visual inspection in MOE was used to identify the interaction between ligand and protein.

All molecular dynamics simulations were performed and analysed using the GROMACS 4.5 simulation package.[41] The Amber99 force field was used. Parameters of the ligands were built using the ANTECHAMBER tool of Amber tools. The Amber forcefield parameters of haem group reported by Akifumi *et al.* were used.[42] The initial structure of each ligand, chosen as best result from docking studies, either free in solution or in complex with the enzyme, was placed in a cubic box with TIP 3P water and consequently energy minimised using a steepest descent minimization algorithm. The system was equilibrated via a 100 ps MD simulation at 300K a NVT canonical environment then an

additional 100 ps simulation at constant pressure of 1 atm was performed (NPT). After the equilibration phases, a 5 ns MD simulation was performed at constant temperature (300 K) and pressure with a time step of 2 fs. Electro-static and Van der Waals ligand-surrounding energies were stored, from MD simulations of the ligands in complex with the enzyme and when free in solution every 3 ps, together with their spatial coordinates, for further analysis.

The estimate $\Delta G_{binding}$ was calculated using GROMACS g_lie function based on LIE equation.[43,44] The method requires the calculation of average interaction energies between the ligand and its surroundings from molecular dynamics (MD) simulations of the ligand free in solution and when bound to the enzyme.

Chemistry. *General Method - Synthesis of Carboxamide Derivatives* (**6** and **10**). To a suspension of carboxylic acid (**4** or **9**) (5 mmol) in anhydrous DMF (5 mL) was added 1,1'-carbonyldiimidazole (5 mmol) and the reaction stirred at room temperature for 1 h. The reaction was cooled to 0 °C and subsequently combined with a solution of 2-amino-1-phenyl-ethanol (**5**) (5 mmol) in DMF (5 mL). The mixture was stirred at room temperature for 8 h. After the reaction was complete, an aliquot amount of ice was poured into the flask to precipitate out the product, which was then filtered, washed with ice-cold H_20 and dried under vacuum with phosphorus pentoxide.

*N-(2-Hydroxy-2-phenylethyl)-4-[(E)-2-(4-fluorophenyl)vinyl]benzamide (**6b**).* A white solid was obtained. Yield: 83 %, R_f 0.88 (petroleum ether – EtOAc 1:3 v/v); m.p. 200-202 ^oC; ^{1}H-NMR (DMSO-d_6): δ 8.53 (t, J = 5.2 Hz, 1H, NH), 7.87 (d, J = 8.2 Hz, 2H, Ar), 7.76-7.70 (m, 4H, Ar), 7.22-7.40 (m, 9H, Ar and alkene), 5.54 (bs, 1H, OH), 4.81 (dd, J = 5.8, 7.9 Hz, 1H, C<u>H</u>OH), 3.49-3.53 (m, 1H, NHC<u>H</u>$_2$), 3.31-3.37 (m, 1H,

NHC$\underline{H}_2$). ^{13} C-NMR (DMSO-d_6): δ 166.0 (C=O), 162.8, 160.9, 143.8, 139.7, 133.4, 133.4, 133.3 (C, Ar), 130.3, 128.9, 128.6, 128.5, 128.0, 127.7, 127.4, 127.0, 126.1, 126.0, 115.7, 115.5 (CH, Ar), 71.2 (CH, $\underline{C}$H-OH), 47.7 (CH_2). Anal. Calcd. for $C_{23}H_{20}O_2FN \bullet 0.1H_2O$ (363.22): C, 76.06 %, H, 5.61 %, N, 3.86 %. Found: C, 75.88 %, H, 5.48 %, N, 3.59 %.

*N-(2-Hydroxy-2-phenylethyl)-4-[(E)-2-(4-methoxyphenyl)vinyl]benzamide (**6c**).* A white solid was obtained. Yield: 74 %, R_f 0.58 (petroleum ether – EtOAc 1:3 v/v); m.p. 230-232 ^{o}C; ^{1}H-NMR (DMSO-d_6): δ 7.86 (t, J = 5.5 Hz, 1H, NH), 7.64 (d, J = 8.2 Hz, 2H, Ar), 7.58 (d, J = 8.6 Hz, 2H, Ar), 7.24-7.40 (m, 6H, Ar and alkene), 7.13-7.16 (m, 1H, Ar), 6.97 (d, J = 8.6 Hz, 2H, Ar), 5.54 (bs, 1H, OH), 4.81 (dd, J = 4.8, 8.0 Hz, 1H, C$\underline{H}$OH), 3.79 (s, 3H, OCH_3), 3.32-3.54 (m, 2H, NHC$\underline{H}_2$). ^{13} C-NMR (DMSO-d_6): δ 166.1 (C=O), 159.3, 140.8, 140.1, 132.8, 130.2 (C, Ar), 130.6, 129.8, 129.4, 128.4, 127.0, 126.0, 125.8, 125.2, 114.2 (CH, Ar), 71.2 (CH, $\underline{C}$H-OH), 55.4 (CH_3), 47.7 (CH_2). Anal. Calcd. for $C_{24}H_{23}O_3N \bullet 0.3H_2O$ (378.86): C, 76.09 %, H, 6.28 %, N, 3.70 %. Found: C, 75.78 %, H, 6.22 %, N, 3.43 %.

*N-(2-Hydroxy-2-phenylethyl)-4-[(E)-2-(3,5-dimethoxyphenyl)vinyl]benzamide (**6d**).* A white solid was obtained. Yield: 75 %, R_f 0.66 (petroleum ether – EtOAc 1:3 v/v); m.p. 168-170 ^{o}C; ^{1}H-NMR (DMSO-d_6): δ 8.52 (t, J = 5.3 Hz, 1H, NH), 7.87 (d, J = 8.3 Hz, 2H, Ar), 7.68 (d, J = 8.3 Hz, 2H, Ar), 7.39 (d, J = 7.3 Hz, 2H, Ar), 7.35 (d, J = 7.4 Hz, 2H, Ar), 7.24-7.33 (m, 3H, Ar and alkene), 6.84 (d, J = 2.0 Hz, 2H, Ar), 6.46 (t, J = 2.0 Hz, 1H, Ar), 5.53 (d, J = 4.0Hz, 1H, OH), 4.81 (dd, J = 4.8, 8.3 Hz, 1H, C$\underline{H}$OH), 3.79 (s, 6H, 2 x OCH_3), 3.49-3.54 (m, 1H, NHC$\underline{H}_2$), 3.34-3.37 (m, 1H, NHC$\underline{H}_2$). ^{13} C-NMR (DMSO-d_6): δ 166.0 (C=O), 160.7, 143.8, 139.6, 138.8, 133.3 (C, Ar), 130.7, 128.1, 128.0, 127.7,

127.0, 126.2, 126.0, 104.7, 100.2 (CH, Ar), 71.2 (CH, CH-OH), 55.2 (2 x OCH_3), 47.7 (CH_2). Anal. Calcd. for $C_{25}H_{25}O_4N$ (403.47): C, 74.42 %, H, 6.25 %, N, 3.47 %. Found: C, 74.25 %, H, 6.52 %, N, 3.72 %.

*N-(2-Hydroxy-2-phenylethyl)-4-[(E)-2-(3,4,5-trimethoxyphenyl)vinyl]benzamide (**6e**).* A white solid was obtained. Yield: 75 %, R_f 0.61 (petroleum ether – EtOAc 1:3 v/v); m.p. 166-168 °C; ^{1}H-NMR (DMSO-d_6): δ 8.50 (t, J = 5.5 Hz, 1H, NH), 7.87 (d, J = 8.2 Hz, 2H, Ar), 7.66 (d, J = 8.2 Hz, 2H, Ar), 7.24-7.40 (m, 7H, Ar and alkene), 6.97 (s, 2H, Ar), 5.34 (bs, 1H, OH), 4.81 (bs, 1H, CHOH), 3.85 (s, 6H, 2 x OCH_3), 3.70 (s, 3H, OCH_3), 3.36-3.53 (m, 2H, $NHCH_2$). ^{13} C-NMR (DMSO-d_6): δ 166.0 (C=O), 153.06, 143.8, 139.9, 137.7, 133.1, 132.5 (C, Ar), 130.3, 128.0, 127.8, 127.0, 126.9, 126.0, 104.2, (CH, Ar), 71.2 (CH, CH-OH), 60.1 (OCH_3), 55.9 (2 x OCH_3), 47.7 (CH_2). HRMS (EI) m/z Calcd for $C_{26}H_{28}NO_5$ $(M+H)^+$ 434.1962. Found 434.1961.

*N-(2-Hydroxy-2-phenyl-ethyl)-4-phenylsulfamoyl-benzamide **(10).*** A white solid was obtained. Yield: 94 %, R_f 0.55 (petroleum ether – EtOAc 1:3 v/v); m.p. 200-202 °C; ^{1}H-NMR (DMSO-d_6): δ 10.31 (bs, 1H, $NHSO_2R$), 8.73 (t, J = 5.7 Hz, 1H, NH), 7.93 (d, J = 8.6 Hz, 2H, Ar), 7.82 (d, J = 8.6 Hz, 2H, Ar), 7.32-7.37 (m, 4H, Ar), 7.22-7.26 (m, 3H, Ar), 7.09 (m, 2H, Ar), 7.04 (m, 1H, Ar), 5.51 (d, J = 4.3 Hz, 1H, OH), 4.75 (m, 1H, CHOH), 3.46 (m, 1H, $NHCH_2$), 3.30 (m, 1H, $NHCH_2$). ^{13} C-NMR (DMSO-d_6): δ 165.1 (C=O), 143.5, 141.5, 138.3, 137.4 (C, Ar), 129.1, 128.0, 128.0, 127.0, 126.6, 125.9, 124.2, 120.2 (CH, Ar), 70.9 (CH, CH-OH), 47.7 (CH_2). Anal. Calcd. for $C_{21}H_{20}O_4N_3S$ (396.45): C, 63.62 %, H, 5.08 %, N, 7.06 %. Found: C, 63.45 %, H, 5.11 %, N, 7.16 %.

*General Method - Synthesis of 4,5-dihydro-1,3-oxazole Derivatives (**7** and **11**).* To

a cooled (0 °C) solution of carboxamide (**6** or **10**) (3 mmol) in anhydrous THF (20 mL) was added methanesulfonyl chloride (24 mmol) and the mixture stirred at 0 °C for 3 h, Then triethylamine (36 mmol) was added dropwise and the reaction stirred at room temperature overnight. The mixture was quenched by the addition of aqueous ammonia solution (28 %, 1 mL). After stirring at room temperature for 15 min the mixture was concentrated *in vacuo* and finally distributed between ethyl acetate (150 mL) and H_2O (2 x 100 mL). After repeated extraction the organic phases were dried and evaporated *in vacuo*.

*(E)-2-(4-(4-Fluorostyryl)phenyl)-5-phenyl-4,5-dihydrooxazole (**7b**).* A white solid was obtained after purification by flash column chromatography (petroleum ether – ethyl acetate 100:0 v/v increasing to 70:30 v/v). Yield: 87 %, R_f 0.86 (petroleum ether – EtOAc 1:3 v/v); m.p. 148-150 ^{o}C; ^{1}H-NMR (DMSO-d_6): δ 7.94 (d, J = 8.3 Hz, 2H, Ar), 7.68-7.72 (m, 4H, Ar), 7.22-7.43 (m, 9H, Ar and alkene), 5.77 (dd, $J_{x,a}$ = 7.7 Hz, $J_{x,b}$ = 10.2 Hz, 1H, CH_x), 4.45 (dd, $J_{b,x}$ = 10.2 Hz, $J_{b,a}$ = 14.7 Hz, 1H, CH_b), 3.85 (dd, $J_{a,x}$ = 7.7 Hz, $J_{a,b}$ = 14.7 Hz, 1H, CH_a). ^{13}C-NMR (DMSO-d_6): δ 162.8, 162.2, 160.9, 141.3, 140.1, 133.3, 126.1 (C), 129.2, 128.7, 128.7, 128.6, 128.2, 128.1, 127.4. 126.6, 125.6, 115.7, 115.6 (CH), 80.1 (CH, oxazole), 62.6 (CH_2 oxazole). Anal. Calcd. for $C_{23}H_{18}NOF \bullet 0.2H_2O$ (347.00): C, 79.61 %, H, 5.34 %, N, 4.04 %. Found: C, 79.51 %, H, 5.43 %, N, 3.75 %.

*(E)-2-(4-(4-Methoxystyryl)phenyl)-5-phenyl-4,5-dihydrooxazole (**7c**).* A pale yellow solid was obtained after purification by flash column chromatography (petroleum ether – ethyl acetate 100:0 v/v increasing to 80:20 v/v). Yield: 42 %, R_f 0.77 (petroleum ether – EtOAc 1:3 v/v); m.p. 160-162 ^{o}C; ^{1}H-NMR (DMSO-d_6): δ 7.92 (d, J = 8.3 Hz, 2H, Ar), 7.68 (d, J = 8.3 Hz, 2H, Ar), 7.59 (d, J = 8.8 Hz, 2H, Ar), 7.32-7.43 (m, 5H, Ar),

7.16 (d, J = 16.7 Hz, 1H, alkene), 7.17 (d, J = 16.6 Hz, 1H, alkene), 6.97 (d, J = 8.8 Hz, 2H, Ar), 5.80 (dd, $J_{x,a}$ = 7.6 Hz, $J_{x,b}$ = 10.1 Hz, 1H, CH_x), 4.45 (dd, $J_{b,x}$ = 10.1 Hz, $J_{b,a}$ = 14.9 Hz, 1H, CH_b), 3.84 (dd, $J_{a,x}$ = 7.5 Hz, $J_{a,b}$ = 14.9 Hz, 1H, CH_a), 3.79 (s, 3H, OCH_3). ^{13}C-NMR (DMSO-d_6): δ 162.3, 159.3, 141.3, 140.6, 129.3, 125.6 (C), 130.1, 128.7, 128.2, 128.1, 128.1, 125.6, 125.1, 114.2, 113.8 (CH), 80.0 (CH, oxazole), 62.6 (CH_2 oxazole), 55.2 (OCH_3). Anal. Calcd. for $C_{24}H_{21}NO_2$ (355.43): C, 81.10 %, H, 5.95 %, N, 3.94 %. Found: C, 81.14 %, H, 6.30 %, N, 3.75 %.

*(E)-2-(4-(3,5-Dimethoxystyryl)phenyl)-5-phenyl-4,5-dihydrooxazole (**7d**).* A yellow oil was obtained after purification by flash column chromatography (petroleum ether – ethyl acetate 100:0 v/v increasing to 70:30 v/v). Yield: 77 %, R_f 0.60 (petroleum ether – EtOAc 1:3 v/v); ^{1}H-NMR ($CDCl_3$): δ 8.03 (d, J = 8.4 Hz, 2H, Ar), 7.59 (d, J = 8.4 Hz, 2H, Ar), 7.36-7.43 (m, 5H, Ar), 7.16 (d, J = 16.4 Hz, 1H, alkene), 7.12 (d, J = 16.4 Hz, 1H, alkene), 6.71 (d, J = 2.2 Hz, 2H, Ar), 6.45 (t, J = 2.2 Hz, 1H, Ar), 5.69 (dd, $J_{x,a}$ = 8.1 Hz, $J_{x,b}$ = 10.2 Hz, 1H, CH_x), 4.51 (dd, $J_{b,x}$ = 10.2 Hz, $J_{b,a}$ = 14.7 Hz, 1H, CH_b), 4.03 (dd, $J_{a,x}$ = 8.0 Hz, $J_{a,b}$ = 14.7 Hz, 1H, CH_a), 3.86 (s, 6H, 2 x OCH_3). ^{13}C-NMR ($CDCl_3$): δ 163.9, 161.1, 141.0, 140.3, 138.9, 126.6 (C), 130.5, 128.8, 128.7, 128.3, 128.3, 126.5, 125.8, 104.8, 100.5 (CH), 81.1 (CH, oxazole), 63.2 (CH_2 oxazole), 55.4 (2 x OCH_3). HRMS (EI) m/z Calcd for $C_{25}H_{24}NO_3$ $(M+H)^+$ 386.1751. Found 381.1753.

*(E)-2-(4-(3,4,5-Trimethoxystyryl)phenyl)-5-phenyl-4,5-dihydrooxazole (**7e**).* A yellow solid was obtained after purification by flash column chromatography (petroleum ether – ethyl acetate 100:0 v/v increasing to 70:30 v/v). Yield: 55 %, R_f 0.75 (petroleum ether – EtOAc 1:3 v/v); m.p. 120-122 ^{o}C; ^{1}H-NMR ($CDCl_3$): δ 8.03 (d, J = 8.3 Hz, 2H, Ar), 7.59 (d, J = 8.3 Hz, 2H, Ar), 7.36-7.43 (m, 5H, Ar), 7.16 (d, J = 16.2 Hz, 1H,

alkene), 7.06 (d, J = 16.2 Hz, 1H, alkene), 6.78 (s, 2H, Ar), 5.69 (dd, $J_{x,a}$ = 8.0 Hz, $J_{x,b}$ = 10.1 Hz, 1H, CH_x), 4.51 (dd, $J_{b,x}$ = 10.1 Hz, $J_{b,a}$ = 14.9 Hz, 1H, CH_b), 4.03 (dd, $J_{a,x}$ = 8.0 Hz, $J_{a,b}$ = 14.9 Hz, 1H, CH_a), 3.97 (s, 3H, OCH_3), 3.94 (s, 6H, 2 x OCH_3). ^{13}C-NMR ($CDCl_3$): δ 163.8, 153.5, 141.1, 140.3, 138.4, 132.6, 126.5 (C), 130.5, 128.8, 128.7, 128.3, 127.3, 126.3, 125.8, 103.9 (CH), 81.1 (CH, oxazole), 63.2 (CH_2 oxazole), 61.0 (OCH_3), 56.2 (2 x OCH_3). Anal. Calcd. for $C_{26}H_{35}NO_4$•0.1H_2O (417.29): C, 74.84 %, H, 6.04 %, N, 3.36 %. Found: C, 74.53 %, H, 6.01 %, N, 3.41 %.

*N-Methanesulfonyl-N-phenyl-4-(5-phenyl-4,5-dihydro-oxazol-2-yl)-benzene sulfonamide (**11**).* A white solid was obtained after purification by flash column chromatography (petroleum ether – ethyl acetate 100:0 v/v increasing to 50:50 v/v). Yield: 55 %, R_f 0.56 (petroleum ether – EtOAc 1:1 v/v); m.p. 148-150 ^{o}C; ^{1}H-NMR (DMSO-d_6): δ 8.18 (d, J = 8.5 Hz, 2H, Ar), 7.96 (d, J = 8.5 Hz, 2H, Ar), 7.50 (t, J = 7.5 Hz, 1H, Ar), 7.43-7.47 (m, 4H, Ar), 7.38-7.40 (m, 3H, Ar), 7.18 (d, J = 7.6 Hz, 2H, Ar), 5.74 (dd, $J_{x,a}$ = 8.2 Hz, $J_{x,b}$ = 10.3 Hz, 1H, CH_x), 4.55 (dd, $J_{b,x}$ = 10.3 Hz, $J_{b,a}$ = 15.3 Hz, 1H, CH_b), 4.08 (dd, $J_{a,x}$ = 8.2 Hz, $J_{a,b}$ = 15.3 Hz, 1H, CH_a $HC\underline{H}_2$), 3.55 (s, 3H, -$SO_2C\underline{H}_3$). ^{13} C-NMR (DMSO-d_6): δ 162.4, 140.6, 140.3, 133.6, 132.9 (C, Ar), 131.1, 130.5, 129.5, 128.9, 128.7, 128.6, 125.7 (CH, Ar), 81.7 (CH, $\underline{C}$H-OH), 63.3 (CH_2), 43.9 (CH_3). Anal. Calcd. for $C_{22}H_{20}O_5N_2S_2$ •0.1H_2O (457.88): C, 57.27 %, H, 4.44 %, N, 6.11 %. Found: C, 57.23 %, H, 4.62 %, N, 6.13.

*General Method - synthesis of Imidazole Derivatives (**8** and **12**).* A mixture of oxazole (**7** or **11**) (1 mmol) and imidazole (40 mmol) dissolved in isopropyl acetate (5 mL) was heated at 125 °C for 48 h. After completion of the reaction the mixture was partitioned between water (100 mL) and ethyl acetate (150 mL). The organic layer was washed three

times with water (3 x 100 mL), dried over $MgSO_4$ and concentrated *in vacuo*.

(E)-N-(2-(1H-imidazol-1-yl)-2-phenylethyl)-4-(4-fluorostyryl)benzamide ***(8b)***. Purification by flash column chromatography (CH_2Cl_2 – MeOH 97:3 v/v) gave a pale yellow solid. Yield: 74 %, R_f 0.60 (CH_2Cl_2 – MeOH 9:1 v/v); m.p. 192-194 ^oC; ^1H-NMR (DMSO-d_6): δ 8.69 (t, J = 5.3 Hz 1H, NH), 7.84 (s, 1H, imid), 7.76 (d, J = 8.3 Hz, 2H, Ar), 7.65-7.69 (m, 5H, Ar and imid), 7.33-7.39 (m, 6H, Ar), 7.21-7.26 (m, 3H, Ar), 6.91 (s, 1H, imid), 5.66 (dd, $J_{x,b}$ = 6.0 Hz, $J_{x,a}$ = 9.3 Hz, 1H, CH_x), 4.03-4.10 (m, 1H, CH_b), 3.94-3.99 (m, 1H, CH_a). ^{13}C-NMR (DMSO-d_6): δ 166.3 (C=O), 162.8, 160.9, 139.9, 139.3, 133.3, 132.8 (C), 136.8, 129.1, 128.7, 128.6, 128.6, 128.1, 128.1, 127.6, 127.4, 126.8, 126.2, 118.3, 115.7, 115.5 (CH), 59.4 (CH), 43.5 (CH_2). Anal. Calcd. for $C_{26}H_{22}N_3OF•0.3H_2O$ (416.88): C, 74.90 %, H, 5.46 %, N, 10.08 %. Found: C, 74.79 %, H, 5.48 %, N, 10.40 %.

(E)-N-(2-(1H-imidazol-1-yl)-2-phenylethyl)-4-(4-methoxystyryl)benzamide ***(8c)***. Purification by flash column chromatography (CH_2Cl_2 – MeOH 97:3 v/v) gave a white solid. Yield: 30 %, R_f 0.66 (CH_2Cl_2 – MeOH 9:1 v/v); m.p. 188-190 ^oC; ^1H-NMR (DMSO-d_6): δ 8.69 (t, J = 5.3 Hz 1H, NH), 7.85 (s, 1H, imid), 7.74 (d, J = 8.4 Hz, 2H, Ar), 7.62 (d, J = 8.4 Hz, 2H, Ar), 7.52 (d, J = 8.6 Hz, 2H, Ar), 7.38 (m, 5H, Ar and imid), 7.28-7.33 (m, 2H, Ar and alkene), 7.13 (d, J = 16.6 Hz, 1H, alkene), 6.96 (d, J = 8.6 Hz, 2H, Ar), 6.92 (s, 1H, imid), 5.68 (dd, $J_{x,b}$ = 5.7 Hz, $J_{x,a}$ = 9.1 Hz, 1H, CH_x), 4.03-4.10 (m, 1H, CH_b), 3.94-3.99 (m, 1H, CH_a), 3.78 (s, 3H, OCH_3). ^{13}C-NMR (DMSO-d_6): δ 166.3 (C=O), 159.3, 140.4, 139.3, 132.3, 129.3 (C), 130.0, 129.9, 128.7, 128.4, 128.3, 128.1, 127.6, 126.8, 125.9, 125.1, 114.2, 113.8 (CH), 59.5 (OCH_3), 55.2 (CH), 43.4 (CH_2). HRMS (EI) m/z Calcd for $C_{27}H_{26}N_3O_2$ $(M+H)^+$ 424.2020. Found 424.2021.

*(E)-N-(2-(1H-imidazol-1-yl)-2-phenylethyl)-4-(3,5-dimethoxystyryl)benzamide (**8d**).* Purification by flash column chromatography (CH_2Cl_2 – MeOH 97:3 v/v) gave a white solid. Yield: 62 %, R_f 0.46 (CH_2Cl_2 – MeOH 9:1 v/v); m.p. 210-212 ^oC; ^1H-NMR (DMSO-d_6): δ 8.73 (t, J = 5.5 Hz 1H, NH), 7.84 (s, 1H, imid), 7.72 (d, J = 8.4 Hz, 2H, Ar), 7.66 (d, J = 8.4 Hz, 2H, Ar), 7.38-7.40 (m, 5H, Ar and imid), 7.27-7.35 (m, 5H, Ar and alkene), 6.91 (s, 1H, imid), 6.81 (d, J = 2.0 Hz, 2H, Ar), 6.45 (t, J = 2.0 Hz, 1H, Ar), 5.68 (dd, $J_{x,b}$ = 5.7 Hz, $J_{x,a}$ = 9.4 Hz, 1H, CH_x), 4.05-4.11 (m, 1H, CH_b), 3.95-4.00 (m, 1H, CH_a), 3.79 (s, 6H, 2 x OCH_3). ^{13}C-NMR (DMSO-d_6): δ 166.3 (C=O), 160.7, 139.9, 139.3, 138.7, 132.8 (C), 136.8, 130.2, 128.7, 128.5, 128.1, 128.0, 127.6, 126.8, 126.3, 118.3, 104.7, 100.3 (CH), 59.4 (2 x OCH_3), 55.2 (CH), 43.4 (CH_2). Anal. Calcd. for $C_{28}H_{27}N_3O_3$•$0.1H_2O$ (455.34): C, 73.86 %, H, 5.98 %, N, 9.23 %. Found: C, 73.61 %, H, 5.61 %, N, 9.18 %.

*(E)-N-(2-(1H-imidazol-1-yl)-2-phenylethyl)-4-(3,4,5-trimethoxystyryl)benzamide (**8e**).* Purification by flash column chromatography (CH_2Cl_2 – MeOH 96:4 v/v) gave a white solid. Yield: 71 %, R_f 0.48 (CH_2Cl_2 – MeOH 9:1 v/v); m.p. 96-98 ^oC; ^1H-NMR (DMSO-d_6): δ 8.72 (t, J = 5.4 Hz 1H, NH), 7.84 (s, 1H, imid), 7.77 (d, J = 8.3 Hz, 2H, Ar), 7.65 (d, J = 8.3 Hz, 2H, Ar), 7.28-7.39 (m, 8H, Ar and imid and alkene), 6.96 (s, 2H, Ar), 6.91 (s, 1H, imid), 5.68 (dd, $J_{x,b}$ = 5.8 Hz, $J_{x,a}$ = 9.4 Hz, 1H, CH_x), 4.05-4.11 (m, 1H, CH_b), 3.95-4.00 (m, 1H, CH_a), 3.96 (s, 3H, OCH_3), 3.84 (s, 6H, 2 x OCH_3). ^{13}C-NMR (DMSO-d_6): δ 166.3 (C=O), 153.1, 140.1, 139.3, 137.7, 132.6, 132.4 (C), 136.8, 130.5, 128.7, 128.5, 128.1, 127.7, 126.8, 126.8, 126.0, 118.3, 104.2 (CH), 60.1 (OCH_3), 55.4 (2 x OCH_3), 55.9 (CH), 43.5 (CH_2). Anal. Calcd. for $C_{29}H_{29}N_3O_4$•$0.3H_2O$ (488.97): C, 71.24 %, H, 6.10 %, N, 8.59 %. Found: C, 70.95 %, H, 5.78 %, N, 8.64 %.

*N-(2-(1H-imidazol-1-yl)-2-phenylethyl)-4-phenyl sulfonyl-benzamide (**12**).* Purification by flash column chromatography (CH_2Cl_2 – MeOH 90:10 v/v) gave a white solid. Yield: 18 %, R_f 0.74 (CH_2Cl_2 – MeOH 9:1 v/v); m.p. 178-180 ^oC; ^1H-NMR (DMSO-d_6): δ 10.35 (bs, 1H, N<u>H</u>SO_2R), 8.90 (t, J = 5.5 Hz, 1H, NH), 7.78-7.85 (m, 5H, Ar and imid), 7.30-7.41 (m, 4H, Ar), 7.33 (m, 2H, Ar), 7.20-7.34 (m, 2H, Ar),7.06-7.09 (m, 2H, Ar and imid), 7.03 (m, 1H, Ar), 6.90 (s, 1H, imid), 5.62 (dd, $J_{x,b}$ = 5.7 Hz, $J_{x,a}$ = 9.5 Hz, 1H, CH_x), 4.02-4.10 (m, 1H, CH_b), 3.93-4.00 (m, 1H, CH_a),. ^{13} C-NMR (DMSO-d_6): δ 165.6 (C=O), 141.7, 139.1, 137.9, 137.3 (C, Ar), 129.1, 128.7, 128.5, 128.0, 126.8, 126.7, 124.3, 120.2, 118.2 (CH), 59.3 (CH), 43.4 (CH_2). HRMS (EI) m/z Calcd for $C_{24}H_{23}O_3N_4$ $(M+H)^+$ 447.1485, Found 447.1476.

*Synthesis of 4-[2-(4-Fluoro-phenyl)-ethyl]-N-(2-imidazol-1-yl-2-phenyl-ethyl)-benzamide (**8f**).* Pd/C catalyst 10% (0.17 g) was added to a solution of compound **8f** (0.2 g, 0.4 mmol) in THF (20 mL) and the reaction was stirred under a H_2 atmosphere for 72 h. After that time the mixture was filtered through celite. The solvent was removed under reduced pressure and the oil formed was purified by flash column chromatography (CH_2Cl_2 - MeOH 100:0 v/v increasing to 98:2 v/v) to give the pure product as white solid. Yield: 52% R_f 0.60 (CH_2Cl_2 – MeOH 9:1 v/v); m.p. 130-132 ^oC; ^1H-NMR (DMSO-d_6): δ 8.63 (t, J = 5.5 Hz 1H, NH), 7.83 (s, 1H, imid), 7.65 (d, J = 8.2 Hz, 2H, Ar), 7.38 (m, 4H, Ar), 7.32 (m, 2H, Ar), 7.27 (d, J = 8.2 Hz, 2H, Ar), 7.23 (m, 2H, Ar and imid), 7.08 (m, 2H, Ar), 6.90 (s, 1H, imid), 5.66 (dd, $J_{x,b}$ = 5.7 Hz, $J_{x,a}$ = 9.7 Hz, 1H, CH_x), 4.04 (m, 1H, CH_b), 3.95 (m, 1H, CH_a), 2.84-2.94 (m, 4H, 2 x CH_2). ^{13}C-NMR (DMSO-d_6): δ 166.5 (C=O), 161.5, 159.6, 144.92, 139.3, 137.27, 131.7 (C), 136.7, 130.1, 130.0, 128.6, 128.4, 128.2, 128.0, 127.1, 126.8, 126.2, 118.3, 114.9, 114.7 (CH), 59.4 (CH), 43.4

(CH_2), 36.7 (CH_2), 35.65 (CH_2). Anal. Calcd. for $C_{26}H_{24}N_3OF \bullet 0.3H_2O$ (418.59): C, 74.60 %, H, 5.92 %, N, 10.03 %. Found: C, 74.26 %, H, 6.22 %, N, 10.00 %.

*Synthesis of1-(4-bromophenyl)-4,4-dimethylpentan-3-one (**15**).* 1-Bromo-4-(bromomethyl)benzene (**13**) (1.95 g, 7.8 mmol) was added to a solution of indium (III) bromide (0.14 g, 0.4 mmol) and 1-(*tert*-butylvinyloxy)trimethylsilane (**14**) (2.7 mL, 12.5 mmol) in CH_2Cl_2 (4 mL). The mixture was stirred for 2 h at room temperature and then poured into aqueous saturated $NaHCO_3$ (100 mL). The resulting mixture was extracted with Et_2O (100 mL), the organic layer dried over $MgSO_4$ and the solvent removed under reduced pressure. Purification by flash column chromatography (petroleum ether - EtOAc 100/0 v/v increasing to 95:5 v/v) gave a yellow oil. Yield: 62 %, R_f 0.74 (petroleum ether – EtOAc 9:1 v/v); ^{1}H-NMR ($CDCl_3$),: δ 7.40 (d, J = 8.4 Hz, 2H, Ar), 7.08 (d, J = 8.4 Hz, 2H, Ar), 2.84 (m, 2H, CH_2), 2.78 (m, 2H, CH_2), 1.11 (s, 9H, 3 x CH_3). ^{13}C-NMR ($CDCl_3$), : δ 214.50, 140.57, 119.75, (C), 131.45, 130.21 (4 x CH), 44.05 (C, *t*Bu), 38.11 (CH_2), 29.40 (CH_2), 26.29 (CH_3 *t*Bu). HRMS (EI) m/z Calcd for $C_{13}H_{18}OBr$ $(M+H)^+$ 269.0536, Found 269.0537.

*General Method – Synthesis of Ketones (**16**).* Vinyl benzene (**2**) (4.5 mmol), 1-(4-bromophenyl)-4,4-dimethylpentan-3-one (**15**) (4.5 mmol) and triethylamine (9 mmol) were heated in the presence of tri(*o*-tolylphosphine) (TOP, 0.16 mmol) and palladium (II) acetate (0.03 mmol) in a sealed tube at 110 ^oC for 6h. After the reaction was complete, water was added (10 mL). The product was partitioned between diethyl ether (100 mL) and water (100 mL), the organic layer dried ($MgSO_4$) and concentrated under reduced pressure.

*4,4-Dimethyl-1-(4-styrylphenyl)pentan-3-one (**16a**).* Purification by flash column chromatography (petroleum ether – EtOAc 95:5 v/v) gave a pale yellow solid. Yield: 78 %, R_f 0.57 (petroleum ether – EtOAc 9:1 v/v); m.p. 70-72 ^{o}C; ^{1}H-NMR ($CDCl_3$): δ 7.53 (d, J = 8.0 Hz 2H, Ar), 7.46 (d, J = 8.1 Hz, 2H, Ar), 7.37 (m, 2H, Ar), 7.28 (m, 1H, Ar), 7.21 (d, J = 7.2 Hz, 2H, Ar), 7.12 (d, J = 16.4 Hz, 1H, alkene), 7.08 (d, J = 16.4 Hz, 1H, alkene), 2.92 (m, 2H, CH_2), 2.83 (m, 2H, CH_2), 1.14 (s, 9H, *t*Bu). ^{13}C-NMR ($CDCl_3$): δ 214.8 (C=O), 141.2, 137.5, 135.2 (C), 128.8, 128.5, 128.3, 128.3, 128.1, 128.0, 126.6 (11 x CH), 44.1 (C, *t*Bu), 38.3 (CH_2), 29.9 (CH_2), 26.3 (CH_3, *t*Bu). HRMS (EI) m/z Calcd for $C_{21}H_{25}O$ $(M+H)^+$ 293.1900. Found 293.1901.

*1-(4-(3,5-Dimethoxystyryl)phenyl)-4,4-dimethylpentan-3-one (**16b**).* Purification by flash column chromatography (petroleum ether – EtOAc 95:5 v/v) gave a pale yellow solid. Yield: 74 %, R_f 0.57 (petroleum ether – EtOAc 9:1 v/v); m.p. 60-62 ^{o}C; ^{1}H-NMR ($CDCl_3$): δ 7.45 (d, J = 8.2 Hz 2H, Ar), 7.20 (d, J = 8.2 Hz, 2H, Ar), 7.08 (d, J = 16.1 Hz, 1H, alkene), 7.02 (d, J = 16.4 Hz, 1H, alkene), 6.69 (d, J = 2.2 Hz, 2H, Ar), 6.42 (t, J = 2.2 Hz, 1H, Ar), 3.85 (s, 6H, 2 x OCH_3), 2.90 (m, 2H, CH_2), 2.83 (m, 2H, CH_2), 1.14 (s, 9H, *t*Bu). ^{13}C-NMR ($CDCl_3$): δ 214.8 (C=O), 161.0, 141.5, 139.5, 135.0 (5 x C), 129.0, 128.9, 128.1, 126.7, 104.5, 99.9 (9 x CH), 55.4 (2 x OCH_3), 44.1 (C, *t*Bu), 38.3 (CH_2), 29.9 (CH_2), 26.3 (CH_3, *t*Bu). HRMS (EI) m/z Calcd for $C_{23}H_{29}O_3$ $(M+H)^+$ 353.2111. Found 353.2114.

*General Method – Synthesis of Alcohols (**17**).* To a cooled solution (0 ^{o}C) of ketone (**16**) (3.4 mmol) in ethanol (60 mL) was added $NaBH_4$ (4.1 mmol) and the reaction stirred at room temperature for 2h. The reaction was concentrated under reduced pressure then 1M aqueous HCl (50 mL) added to the residue. The resulting white oil was extracted with

diethyl ether (2 x 50 mL) and the organic layer back-extracted with water (2 x 25 mL), dried ($MgSO_4$) and concentrated to give the pure compound.

*4,4-Dimethyl-1-(4-styrylphenyl)pentan-3-ol (**17a**).* Obtained as a white solid. Yield: 67 %, R_f 0.41 (petroleum ether – EtOAc 9:1 v/v); m.p. 76-78 ^oC; ^1H-NMR ($CDCl_3$): δ 7.53 (d, J = 7.3 Hz 2H, Ar), 7.47 (d, J = 8.1 Hz, 2H, Ar), 7.37 (m, 2H, Ar), 7.28 (m, 1H, Ar), 7.24 (d, J = 7.9 Hz, 2H, Ar), 7.13 (d, J = 16.2 Hz, 1H, alkene), 7.09 (d, J = 16.2 Hz, 1H, alkene), 3.26 (m, 1H, C<u>H</u>OH), 2.95 (m, 1H, CH_2), 2.67 (m, 1H, CH_2), 1.88 (m, 1H, CH_2), 1.62 (m, 1H, CH_2), 1.43 (d, J = 5.4 Hz, 1H, OH), 0.92 (s, 9H, *t*Bu). ^{13}C-NMR ($CDCl_3$): δ 142.1, 137.5, 135.0 (C), 128.9, 128.7, 128.6, 127.9, 127.5, 126.6, 126.4 (11 x CH), 79.3 (<u>C</u>HOH), 35.1 (C, *t*Bu), 33.3 (CH_2), 33.1 (CH_2), 25.7 (CH_3, *t*Bu). HRMS (EI) m/z Calcd for $C_{21}H_{27}O$ $(M+H)^+$ 295.2056. Found 295.2062.

*1-(4-(3,5-Dimethoxystyryl)phenyl)-4,4-dimethylpentan-3-ol (**17b**).* Obtained as a clear thick syrup. Yield: 83 %, R_f 0.41 (petroleum ether – EtOAc 9:1 v/v); ^1H-NMR ($CDCl_3$): δ 7.47 (d, J = 8.2 Hz 2H, Ar), 7.25 (d, J = 8.2 Hz, 2H, Ar), 7.10 (d, J = 16.3 Hz, 1H, alkene), 7.03 (d, J = 16.3 Hz, 1H, alkene), 6.70 (d, J = 2.2 Hz, 2H, Ar), 6.43 (t, J = 2.2 Hz, 1H, Ar), 3.86 (s, 6H, 2 x OCH_3), 3.26 (d, J = 10.5 Hz, 1H, C<u>H</u>OH), 2.96 (m, 1H, CH_2), 2.67 (m, 1H, CH_2), 1.89 (m, 1H, CH_2), 1.63 (m, 1H, CH_2), 1.55 (bs, 1H, OH), 0.94 (s, 9H, *t*Bu). ^{13}C-NMR ($CDCl_3$): δ 161.0, 142.3, 139.6, 134.8 (C), 129.2, 128.9, 128.2, 126.7, 104.5, 99.9 (9 x CH), 79.3 (<u>C</u>HOH), 55.4 (2 x OCH_3), 35.0 (C, *t*Bu), 33.3 (CH_2), 33.1 (CH_2), 25.7 (CH_3, *t*Bu). HRMS (EI) m/z Calcd for $C_{23}H_{31}O_3$ $(M+H)^+$ 355.2268. Found 355.2258.

Synthesis of 1-(4-(3,5-Dimethoxystyryl)phenyl)-4,4-dimethylpentan-3-yl-1H-imidazole-1-carboxylate (**18b**). To a solution of alcohol **17b** (0.5 g, 1.4 mmol) in dry CH_3CN (20 mL) was added imidazole (0.3 g, 4.2 mmol) and 1,1'-carbonyldiimidazole (0.34 g, 2.1 mmol). The mixture was heated at 70 ^oC for 48 h. After cooling the reaction was extracted between CH_2Cl_2 (50 mL) and H_2O (50 mL), the aqueous layer was further washed with CH_2Cl_2 (2 x 50 mL), then the combined organic layers washed with and H_2O (3 x 50 mL), dried ($MgSO_4$) and concentrated under reduced pressure. Purification by flash column chromatography (petroleum ether – EtOAc 9:1 v/v increasing to 3:2 v/v) gave a thick colourless oil. Yield: 65 %, R_f 0.33 (petroleum ether – EtOAc 7:3 v/v); ^{1}H-NMR ($CDCl_3$): δ 8.17 (s, 1H, imid), 7.46 (m, 3H, Ar + imid), 7.25 (d, J = 8.2 Hz, 2H, Ar), 7.12 (s, 1H, imid), 7.03 (d, J = 16.2 Hz, 1H, alkene), 6.97 (d, J = 16.2 Hz, 1H, alkene), 6.69 (d, J = 2.2 Hz, 2H, Ar), 6.39 (t, J = 2.2 Hz, 1H, Ar), 4.95 (dd, J = 3.0, 9.6 Hz, 1H, C<u>H</u>OC(O)imid), 3.86 (s, 6H, 2 x OCH_3), 2.69 (m, 2H, CH_2), 2.05 (m, 2H, CH_2), 0.94 (s, 9H, *t*Bu). ^{13}C-NMR ($CDCl_3$): δ 161.0, 149.0, 140.6, 139.4, 135.2 (6 x C), 137.0, 130.6, 128.6, 128.3, 128.2, 126.7, 117.1, 104.6, 99.9 (12 x CH), 86.3 (<u>C</u>HOC(O)imid), 55.4 (2 x OCH_3), 32.5 (C, *t*Bu), 35.1 (CH_2), 33.4 (CH_2), 25.8 (CH_3, *t*Bu). HRMS (EI) m/z Calcd for $C_{27}H_{33}N_2O_4$ $(M+H)^+$ 449.2435. Found 449.2431.

*General Method – Synthesis of Sulfonates (**20** and **21**).* To a cooled solution (0 ^oC) of alcohol (**17**) (1.8 mmol) and 4-dimethylaminopyridine (0.4 mmol) in dry CH_2Cl_2 (7 mL) and pyridine (0.7 mL) was added methane sulfonyl chloride or toluene sulfonyl chloride (4 mmol) dropwise. The reaction was stirred at 0 ^oC for 10 min then at room temperature for 24h (mesyl derivative) or reflux for 24 h (tosyl derivative). On completion and

cooling to room temperature (tosyl reaction), the crude reaction mixture was washed with saturated aqueous $NaHCO_3$ (30 mL) and the organic layer separated. The aqueous layer was back extracted with CH_2Cl_2 (30 mL), then the combined organic layers washed with aqueous 1M HCl (30 mL) and saturated aqueous $NaHCO_3$ (30 mL), dried ($MgSO_4$) and concentrated under reduced pressure.

*4,4-Dimethyl-1-(4-styrylphenyl)pentan-3-yl methanesulfonate (**20a**).* Purification by flash column chromatography (petroleum ether – EtOAc 9:1 v/v) gave a white solid. Yield: 52 %, R_f 0.53 (petroleum ether – EtOAc 4:1 v/v); m.p. 80-82 ^oC; ^1H-NMR ($CDCl_3$): δ 7.53 (d, J = 7.6 Hz 2H, Ar), 7.48 (d, J = 8.0 Hz, 2H, Ar), 7.38 (m, 2H, Ar), 7.28 (m, 1H, Ar), 7.24 (d, J = 8.0 Hz, 2H, Ar), 7.12 (d, J = 16.6 Hz, 1H, alkene), 7.09 (d, J = 16.6 Hz, 1H, alkene), 4.58 (t, J = 5.6 Hz, 1H, C<u>H</u>OMs), 3.11 (s, 3H, Ms), 2.97 (m, 1H, CH_2), 2.73 (m, 1H, CH_2), 1.99 (m, 2H, CH_2), 1.01 (s, 9H, *t*Bu). ^{13}C-NMR ($CDCl_3$): δ 141.0, 137.5, 135.3 (C), 128.7, 128.5, 128.2, 127.5, 126.7, 126.6, 126.4 (11 x CH), 91.5 (<u>C</u>HOMs), 38.9 (CH_3, Ms), 35.3 (C, *t*Bu), 32.8 (CH_2), 32.7 (CH_2), 26.2 (CH_3, *t*Bu). HRMS (EI) m/z Calcd for $C_{22}H_{32}NO_3S$ $(M+NH_4)^+$ 390.2097. Found 390.2094..

*1-(4-(3,5-Dimethoxystyryl)phenyl)-4,4-dimethylpentan-3-yl methanesulfonate (**20b**).* Purification by flash column chromatography (petroleum ether – EtOAc 9:1 v/v) gave a yellow oil. Yield: 84 %, R_f 0.53 (petroleum ether – EtOAc 4:1 v/v); ^1H-NMR ($CDCl_3$): δ 7.46 (d, J = 8.2 Hz 2H, Ar), 7.24 (d, J = 8.1 Hz, 2H, Ar), 7.09 (d, J = 16.3 Hz, 1H, alkene), 7.02 (d, J = 16.3 Hz, 1H, alkene), 6.69 (d, J = 2.2 Hz, 2H, Ar), 6.42 (t, J = 2.2 Hz, 1H, Ar), 4.57 (dd, J = 3.1, 5.0 Hz, 1H, C<u>H</u>OMs), 3.85 (s, 6H, 2 x OCH_3), 3.10 (s, 3H, Ms), 2.97 (m, 1H, CH_2), 2.73 (m, 1H, CH_2), 1.98 (m, 2H, CH_2), 1.00 (s, 9H, *t*Bu). ^{13}C-NMR ($CDCl_3$): δ 161.0, 141.1, 139.5, 135.1 (5 x C), 128.9, 128.8, 128.1, 126.7,

104.5, 99.9 (9 x CH), 91.5 (CHOMs), 55.4 (2 x OCH_3), 38.9 (CH_3, Ms), 35.0 (C, *t*Bu), 32.8 (CH_2), 32.7 (CH_2), 26.2 (CH_3, *t*Bu). HRMS (EI) m/z Calcd for $C_{24}H_{33}SO_5$ $(M+H)^+$ 433.2043. Found 433.2043.

*1-(4-(3,5-Dimethoxystyryl)phenyl)-4,4-dimethylpentan-3-yl toluenesulfonate (**21b**).* Purification by flash column chromatography (petroleum ether – EtOAc 9:1 v/v) gave a thick colourless oil. Yield: 8 %, R_f 0.37 (petroleum ether – EtOAc 4:1 v/v); ^{1}H-NMR ($CDCl_3$): δ 7.86 (d, J = 8.2 Hz 2H, Ar), 7.44 (d, J = 8.0 Hz 2H, Ar), 7.36 (d, J = 8.0 Hz 2H, Ar), 7.12 (d, J = 8.1 Hz, 2H, Ar), 7.08 (d, J = 16.3 Hz, 1H, alkene), 7.01 (d, J = 16.3 Hz, 1H, alkene), 6.69 (d, J = 2.2 Hz, 2H, Ar), 6.42 (t, J = 2.1 Hz, 1H, Ar), 4.54 (dd, J = 3.1, 5.0 Hz, 1H, CHOTs), 3.85 (s, 6H, 2 x OCH_3), 2.75 (m, 1H, CH_2), 2.61 (m, 1H, CH_2), 2.47 (s, 3H, Ts), 1.93 (m, 2H, CH_2), 0.91 (s, 9H, *t*Bu). ^{13}C-NMR ($CDCl_3$): δ 161.0, 144.2, 141.3, 139.5, 135.4, 135.0 (7 x C), 129.6, 129.0, 128.8, 128.1, 127.5, 126.7, 104.5, 99.9 (13 x CH), 92.2 (CHOTs), 55.4 (2 x OCH_3), 35.4 (C, *t*Bu), 32.9 (CH_2), 32.8 (CH_2), 26.2 (CH_3, *t*Bu), 21.6 (CH_3, Ts). HRMS (EI) m/z Calcd for $C_{30}H_{37}SO_5$ $(M+H)^+$ 509.2356. Found 509.2350.

*Synthesis of 2-Imidazol-1-yl-4,4-dimethyl-1-(4-styryl-phenyl)-pent-1-en-3-one (**24**).* To a stirred solution of **22** (0.48 g, 2.8 mmol) and K_2CO_3 (0.48 g, 3.5 mmol) in Ac_2O (8 mL) was added **23** (0.72 g, 3.5 mmol). The mixture was stirred for 3 h at room temperature. After quenched with water (50 mL), the resulting mixture was extracted with EtOAc (50 mL × 4). The combined organic layer was washed with brine (150 mL), dried over $MgSO_4$, and concentrated *in vacuo*. The residual oil was purified by silica gel flash column chromatography (petroleum ether-EtOAc 100:0 v/v increasing to 50:50 v/v) to

obtain the E/Z mixture compound as a yellow solid. Yield: 16 %, R_f 0.65 (petroleum ether – EtOAc 1:1 v/v); m.p. 122-124 ^{o}C; ^{1}H-NMR ($CDCl_3$): δ 7.52 (d, J= 7.4 Hz, 2H, Ar), 7.47 (s, 1H, imid), 7.44 (s, 1H, alkene), 7.36-7.42 (m, 4H, Ar and imid), 7.30 (m, 2H, Ar), 7.15 (d, J = 16.4 Hz, 1H, alkene), 7.04 (d, J = 16.4 Hz, 1H, alkene), 6.94 (s, 1H, imid), 6.77 (d, J = 8.4 Hz, 2H, Ar), 1.25 (s, 9H, *t*Bu). ^{13}C-NMR ($CDCl_3$): δ 203.0 (C=O), 139.7, 136.7, 132.1, 130.6 (5 C), 137.3, 136.4, 130.8, 130.4, 130.3, 128.7, 128.2, 127.37, 126.9, 126.7, 119.7 (CH), 44.1 (C, *t*Bu) 27.8 (CH_3, *t*Bu). Anal. Calcd. for $C_{24}H_{24}N_2O$•0.1H_2O (357.99): C, 80.52 %, H, 6.81 %, N, 7.82 %. Found: C, 80.39 %, H, 6.83 %, N, 7.82 %.

*Synthesis of 2-Imidazol-1-yl-4,4-dimethyl-1-(4phenylethyl)-pentan-3-one (**25**).* Reduction of (**24**) by catalytic reduction following the procedure reported for **8f**. Purification by flash column chromatography (100:0 v/v increasing to 50:50 v/v) gave a white wax. Yield: 40 %, R_f 0.21 (petroleum ether – EtOAc 1:1 v/v); ^{1}H-NMR ($CDCl_3$): δ 7.42 (s, 1H, imid), 7.24-7.31 (m, 2H, Ar and imid), 7.20 (m, 1H, Ar), 7.14 (m, 2H, Ar), 7.30 (m, 2H, Ar), 7.03-7.07 (m, 4H, Ar), 6.87-6.91 (m, 2H, Ar and imid), 5.25 (dd, $J_{x,b}$ = 6.8 Hz, $J_{x,a}$ = 8.4 Hz, 1H, CH_x), 3.24 (m, 1H, CH_b), 3.09 (m, 1H, CH_a), 2.89 (s, 4H, 2 x CH_2), 1.04 (s, 9H, *t*Bu). ^{13}C-NMR ($CDCl_3$): δ 209.6 (C=O), 141.4, 140.8, 133.3 (4 C), 136.5, 129.6, 128.9, 128.9, 128.4, 128.3, 125.9, 117.7 (CH), 60.0 (CH), 44.8 (C, *t*Bu), 39.8, 37.7, 37.3 (CH_2), 25.6 (CH_3, *t*Bu). HRMS (EI) m/z Calcd for $C_{24}H_{29}N_2O$ $(M+H)^+$ 361.2274. Found 361.2269.

AUTHOR INFORMATION

Corresponding author

Tel: +44(0)2920-876307. Fax: +44(0)2920-874149. E-mail: SimonsC@Cardiff.ac.uk

ACKNOWLEDGEMENTS

We acknowledge Cancer Research UK for funding (SF, Grant Ref. C7735/ A10649), the Embassy of the Arab Republic of Egypt (ASA, PhD scholarship) and the EPSRC Mass Spectrometry Centre, Swansea, UK for mass spectroscopy data.

REFERENCES

[1] DeLuca, H.F. Overview of general physiologic features and functions of vitamin D. *Am. J. Clin. Nutr*. **2004**, *80*, 1689S-1696S

[2] Nagpal, S.; Na, S.; Rathnachalam, R. Noncalcemic actions of vitamin D receptor ligands. *Endocrine Rev*. **2005**, *26*, 662-687.

[3] Ylikomi, T.; Laaski, I.; Lou, Y.R.; Martikainen, P.; Pennanen, P.; Purmonen, S.; Syvala, H.; Vienone, A.; Tuolimaa, O. Antiproliferative action of vitamin D. *Vitam. Horm.* **2002**, *64*, 357-406.

[4] Swaimi, S.; Krishnan, A.V.; Feldman, D. Vitamin D metabolism and action in the prostate: implications for health and disease. *Mol. Cell. Endocrinol*. **2011**, *347*, 61-69.

[5] Cross, H.S.; Bises, G.; Lechner, D.; Manhardt, T.; Kallay, E. The vitamin D endocrine system of the gut – its possible role in colorectal cancer prevention. *J. Steroid Biochem. Mol. Biol*. **2005**, *97*, 121-128.

[6] Chen, G.; Kim, S.H.; King, A.N.; Zhao, L.; Simpson, R.U.; Christensen, P.J.; Wang, Z.; Thomas, D.G.; Giorgano, T.J.; Lin, L.; Brenner, D.E.; Beer, G.G.; Ramnath, N.

CYP24A1 is an independent prognostic marker of survival in patients with lung adenocarcinoma. *Clin. Cancer Res*. **2011**, *17*, 817-826.

[7] Cantorna, M.T. Vitamin D, multiple sclerosis and inflammatory bowel disease. *Arch. Biochem. Biophys*. **2012**, *523*, 103-106.

[8] Simon, K.C.; Munger, K.L.; Ascherio, A. Vitamin D and multiple sclerosis: epidemiology, immunology and genetics. *Curr. Opin. Neurol*. **2012**, *25*, 246-251.

[9] Posner, G.H.; Helvig, C.; Cuerrier, D.; Collop, D.; Kharebov, A.; Ryder, K.; Epps, T.; Petkovich, M. Vitamin D analogues targeting CYP24 in chronic kidney disease. *J. Steroid Biochem. Mol. Biol*. **2010**, *121*, 13-19.

[10] Sterling, K.A.; Eftekhari, P.; Girndt, M.; Kimmel, P.L.; Raj, D.S. The immunoregulatory function of vitamin D: implications in chronic kidney disease. *Nature Rev. Nephrol*. **2012**, *8*, 403-412.

[11] Jones, G.; Prosser, D.E.; Kaufman, M. 25-Hydroxy vitamin D-24-hydroxylase (CYP24A1): its important role in the degradation of vitamin D. *Arch. Biochem. Biophys*. **2012**, *523*, 9-18.

[12] Posner, G.H.; Wang, Q.; Han, G.; Lee, J.K.; Crawford, K.; Zand, S.; Brem, H.; Peleg, S.; Dolan, P.; Kensler, T.W. Conceptually new sulfone analogues of the hormone 1alpha, 25-dihydroxyvitamin D_3: synthesis and preliminary biological evaluation. *J. Med. Chem*. **1999**, *42*, 3425-3435.

[13] Kahraman, M.; Sinishtaj, S.; Dolan, P.M.; Kensler, T.W.; Peleg, S.; Saha, U.; Chuang, S.S.; Bernstein, G.; Korczak, B.; Posner, G.H. Potent, selective and low-calcemic inhibitors of CYP24 hydroxylase: 24-sulfoximine analogues of the hormone 1alpha, 25-dihydroxyvitamin D_3. *J. Med. Chem*. **2004**, *47*, 6854-6863.

[14] Zhu, J.; Barycki, R.; Chiellini, G.; DeLuca, H.F. Screening of selective inhibitors of 1α,25-dihydroxyvitamin D_3 24-hydroxylase using recombinant human enzyme expressed in *Escherichia coli*. *Biochem*. **2010**, *49*, 10403-10411.

[15] Chiellini, G.; Rapposelli, S.; Zhu, J.; Massarelli, I.; Saraceno, M.; Bianucci, A.M.; Plum, L.A.; Clagett-Dame, M.; DeLuca, H.F. Synthesis and biological activities of vitamin D-like inhibitors of CYP24 hydroxylase. *Steroids* **2012**, *77*, 212-223.

[16] Schuster, I.; Egger, H.; Nussbaumer, P.; Kroemer, R.T. Inhibitors of vitamin D hydroxylases: structure-activity relationships. *J. Cell. Biochem.* **2003**, *88*, 372-380.

[17] Schuster, I.; Egger, H.; Astecker, N.; Herzig, G.; Schussler, M.; Vorisek, G. Selective inhibitors of CYP24: mechanistic tools to explore vitamin D metabolism in human keratinocytes. *Steroids* **2001**, *66*, 451-462.

[18] Ly, L.H.; Zhao, X.Y.; Holloway, L.; Feldman, D. Liarozole acts synergistically with 1alpha,25-dihydroxyvitamin D3 to inhibit growth of DU 145 human prostate cancer cells by blocking 24-hydroxylase activity. *Endocrinology* **1999**, *140*, 2071-2076.

[19] Aboraia, A.S.; Yee, S.W.; Gomaa, M.S.; Shah, N.; Robotham, A.C.; Makowski, B.; Prosser, D.; Brancale, A.; Jones, G.; Simons, C. Synthesis and CYP24A1 inhibitory activity of *N*-(2-(1*H*-imidazol-1-yl)-2-phenylethyl)arylamides. *Bioorg. Med. Chem*. **2010**, *18*, 4939-4946.

[20] Gehringer, L.; Bourgogne, C.; Guillon, D.; Donnio, B. Liquid crystalline octopus dendrimers: block molecules with unusual mesophase morphologies. *J. Am Chem Soc*. **2004**, *126*, 3856-3867.

[21] Osterod, F.; Peters, L.; Kraft, A.; Sano, A.; Morrison, J.J.; Feeder, N.; Holmes, A.B. Luminescent supramolecular assemblies based on hydrogen-bonded complexes of stilbenecarboxylic acids and dithieno[3,2-*b*:2',3'-*d*]thiophene-2-carboxylic acids with a tris(imidazoline) base. *J. Mat. Chem*. **2001**, *11*, 1625-1633.

[22] Durantini, E.N. Synthesis of meso-nitrophenylporphyrins covalently linked to a polyphenylene chain bearing methoxy groups. *J. Porphyr. Phthalocya*. **2000**, *4*, 233-242.

[23] Nazir, S.; Muhammad, K.; Rauf, M.K.; Ebihara, M.; Hameed, S. (*E*)-4-(4-fluorostyryl)benzoic acid. Acta Crystallogr. Sect. E Struct. Rep. Online, **2008**, E64, O1013-U1606.

[24] Gant. T.G.; Meyers, A.I. The chemistry of 2-oxazolines (1985-present). *Tetrahedron* **1994**, *50*, 2297-2360.

[25] Sund, C.; Ylikoski, J.; Kwiatkowski, M. A new simple and mild synthesis of 2-substituted 2-oxazolines. *Synthesis-Stuttgart* **1987**, 853-854.

[26] Wehrmeister, H.L. Reactions of aromatic thiols with oxazolines. *J. Org. Chem*. **1963**, *28*, 2587-2588.

[27] Zheng, X.; Oda, H.; Takamatsu, K.; Sugimoto, Y.; Tai, A.; Akaho, E.; Ali', H.I.; Oshiki, T.; Kakuta, H.; Sasaki, K. Analgesic agents without gastric damage: design and synthesis of structurally simple benzenesulfonanilide-type cyclooxygenase-1-selective inhibitors. *Bioorg. Med. Chem*. **2007**, *15*, 1014-1021.

[28] Nishimoto, Y.; Saito, T.; Yasuda, M.; Baba, A. Indium-catalyzed coupling reaction between silyl enolates and alkyl chlorides or alkyl ethers. *Tetrahedron* **2009**, *65*, 5462-5471.

[29] Todoroki, Y.; Kobayashi, K.; Yoneyama, H.; Hiramatsu, S.; Jin, M.H.; Watanabe,

B.; Mizutani, M.; Hirai, N. Structure-activity relationship of uniconazole, a potent inhibitor of ABA 8'-hydroxylase, with a focus on hydrophilic functional groups and conformation. *Bioorg. Med. Chem,* **2008**, *16*, 3141-3152.

[30] http://www.ncbi.nlm.nih.gov/geoprofiles?term=GDS4168%5BACCN%5D (Chronic lymphocytic leukemia: peripheral blood B cells (HG-U133B). Accessed 20/8/2014.

[31] Gomaa, M.S.; Brancale, A.; Simons, C. Homology model of 1α,25-dihydroxyvitamin D_3 24-hydroxylase cytochrome P450 24A1 9CYP24A1): active site architecture and ligand binding. *J. Steroid Biochem. Mol. Biol*. **2007**, *104*, 53-60.

[32] Annalora, A.J.; Goodin, D.B.; Hong, W.H.; Zhang, Q.; Johnson, E.F.; Stout, C.D. Crystal structure of CYP24A1, a mitochondrial cytochrome P450 involved in vitamin D metabolism. *J. Mol. Biol*. **2010**, *396*, 441-451.

[33] RAMPAGE Server http://mordred.bioc.cam.ac.uk/~rapper/rampage.php. Accessed 20/8/2014.

[34] Bowie, J.U.; Luthy, R.; Eisenberg, D. A method to identify protein sequences that fold into a known three-dimensional structure. *Science* **1991**, *253*, 164–170

[35] Colovos, C.; Yeates, T.O. Verification of protein structures: patterns of nonbonded atomic interactions. *Protein Sci*. **1993**, *2*, 1511–1519.

[36] Akutsu, N.; Lin, R.; Bastien, Y.; Bestawros, A.; Enepekides, D.J.; Black, M.; White, J.H. Regulation of gene expression by 1α, 25-dihydroxyvitamin D3 and its analog EB1089 under growth-inhibitory conditions in squamous carcinoma cells. *Mol. Endocrinol*. **2001**, *15*, 1127-1139.

[37] Yee, S.W.; Campbell, M.J.; Simons, C. Inhibition of vitamin D3 metabolism enhances VDR signaling in androgen-independent prostate cancer cells. *J. Steroid*

Biochem. Mol. Biol. **2006**, *98*, 228-235.

[38] Perrin D.D.; Armarengo, W.L.F. Purification of laboratory chemicals, 3rd Ed.: Pergamon Press: New York, 1988

[39] LeadIT. http://www.biosolveit.de/. Accessed 20/8/2014.

[40] Molecular operating Environment. http://www.chemcomp.com/MOE-Molecular_Operating_Environment.htm. Accessed 20/8/2014.

[41] Hess, B.; Kutzner, C.; Van der Spoel, D.; Lindahl, E. Algorithms for highly efficient, load-balanced, and scalable molecular simulation *J. Chem. Theory Comput.* **2008**, *4*, 435-447.

[42] Oda, A.; Yamaotsu, N.; Hirono, S. New AMBER force field parameters of heme iron for cytochrome P450s determined by quantum chemical calculation of simplified models. *J. Comput. Chem*. **2005**, *26*, 818-826.

[43] Vasanthanathan, P.; Olsen, L.; Jørgensen F. S.; Vermeulen, N. P. E.; Oostenbrink C. Computational prediction of binding affinity for CYP1A2-ligand complexes using empirical free energy calculations. *Drug Metab. Dispos*.. **2010**, *38*, 1347-1354.

[44] Hansson, T.; Marelius, J.; Åqvist, J. Ligand binding affinity prediction by linear interaction energy methods. *J. Comput. Aid. Mol. Des*. **1998**, *12*, 27–35.

Table of Contents Graphic